JARA|FIT

JÜLICH FORSCHUNGSZENTRUM

RWTH AACHEN UNIVERSITY

SFB 917 Nanoswitches

Modeling of ReRAMs based on the Valence Change Mechanism: From Atomistic to Circuit-Level Models

S. Menzel[1]

[1]Peter Grünberg Institut (PGI-7), Forschungszentrum Jülich, Germany

IEEE International Memory Workshop, 21st of May 2023

Redox-based Memristive Devices

Resistive Switching,
Edited by D. Ielmini, R. Waser
Wiley-VCH 2016

ElectroChemical Metallization Cells

- also called CBRAM or Atomic Switch
- bipolar
- filamentary

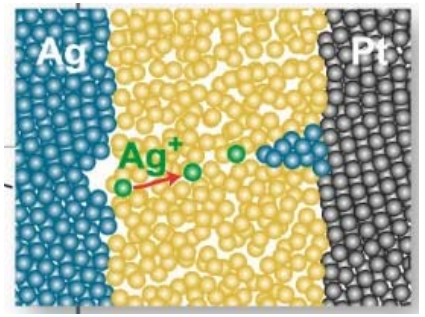

Valence Change Mechanism Cells

- also OxRAM or RRAM
- bipolar
- filamentary and non-filamentary

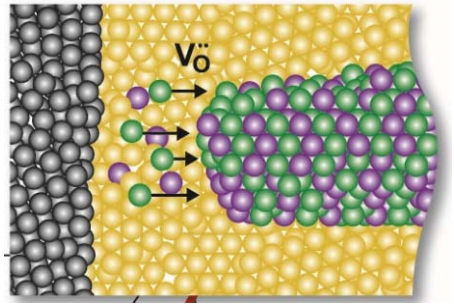

ThermoChemical Mechanism Cells

- unipolar
- low endurance
- only minor activities

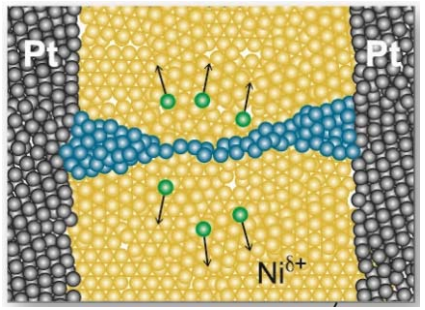

Filamentary VCM Cells: Switching Mechanism

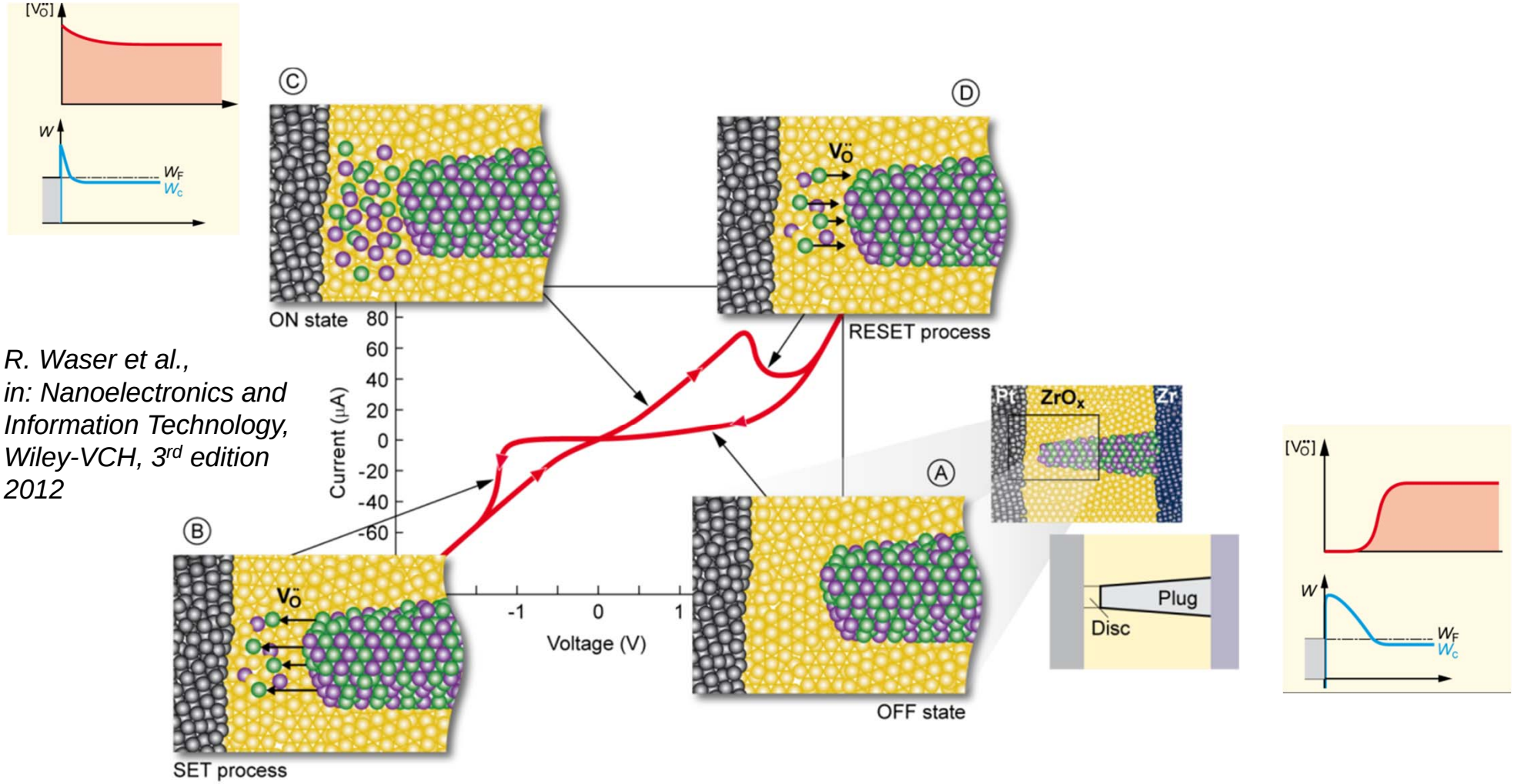

R. Waser et al., in: Nanoelectronics and Information Technology, Wiley-VCH, 3rd edition 2012

→ Processes: ion motion, oxygen exchange, Joule heating

Comprehensive Review Article on VCM Cells

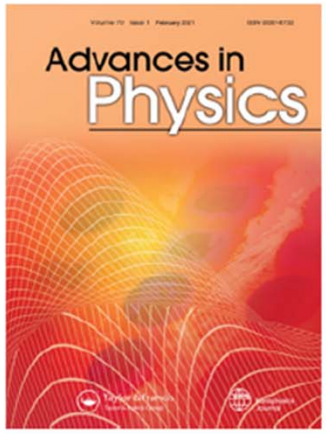

Taylor & Francis
Taylor & Francis Group

Advances in Physics

ISSN: (Print) (Online) Journal homepage: https://www.tandfonline.com/loi/tadp20

Nanoionic memristive phenomena in metal oxides: the valence change mechanism

Regina Dittmann, Stephan Menzel & Rainer Waser

To cite this article: Regina Dittmann, Stephan Menzel & Rainer Waser (2022): Nanoionic memristive phenomena in metal oxides: the valence change mechanism, Advances in Physics, DOI: 10.1080/00018732.2022.2084006

To link to this article: https://doi.org/10.1080/00018732.2022.2084006

Multiscale Modeling

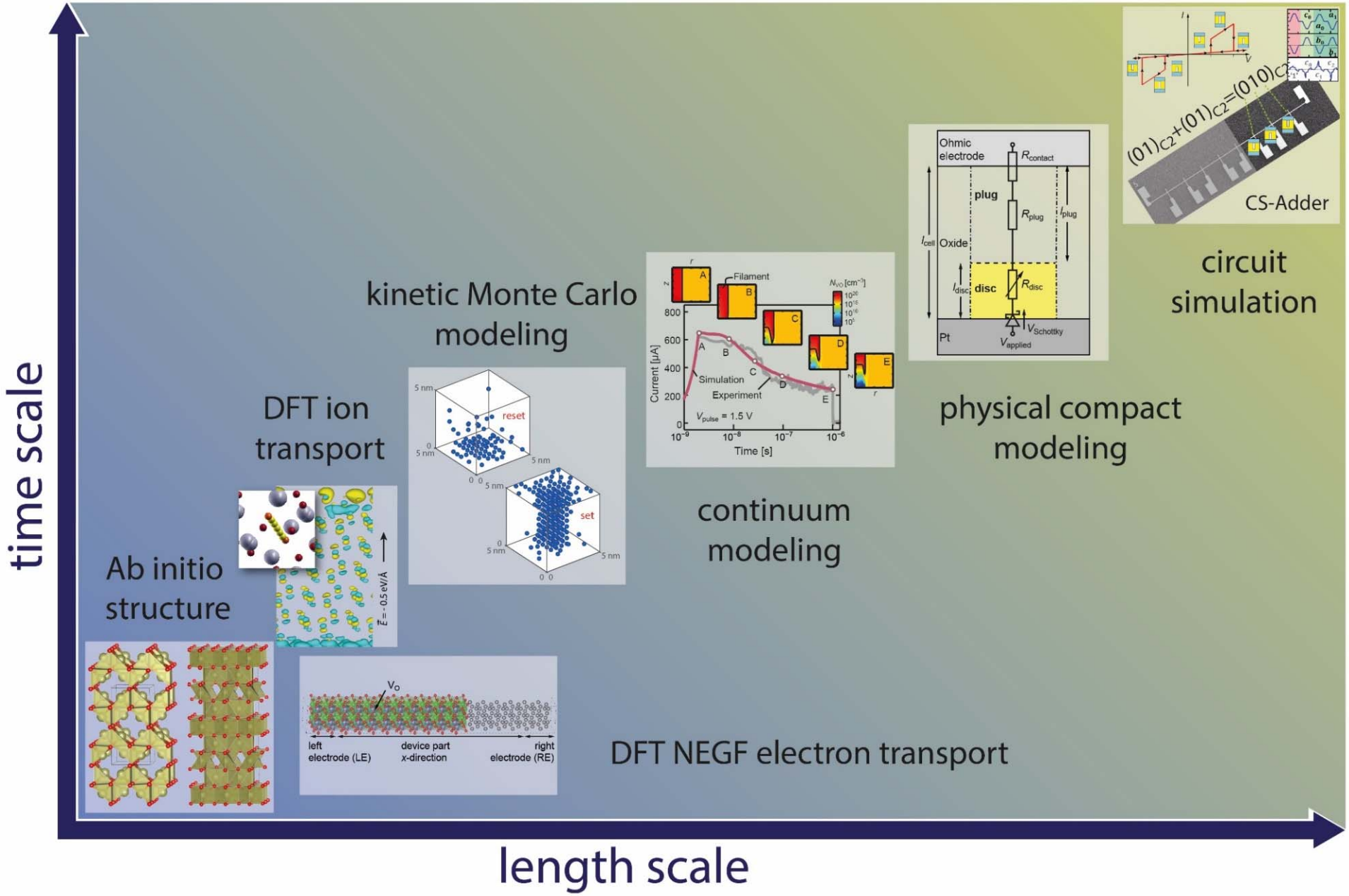

Outline

- Motivation
- **Electronic Transport in VCM Cells: A DFT-NEGF study**
- Switching Variability of VCM Cells: Kinetic Monte Carlo Modeling
- Switching Dynamics of VCM Cells: Continuum Modeling
- Towards Circuit Simulations: VCM Compact Models (JART)
- Array Level Modeling
- Summary & Conclusion

Typical *I-V* Characteristics of VCM Cells

Type I Conduction

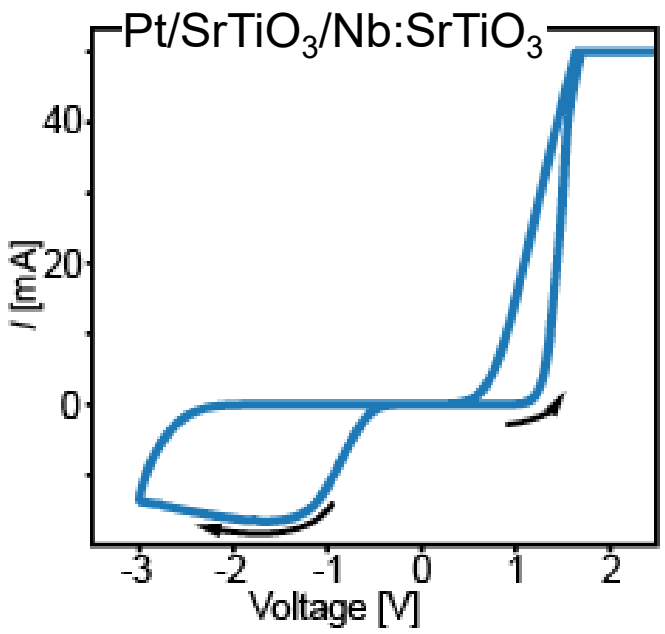

Type II Conduction

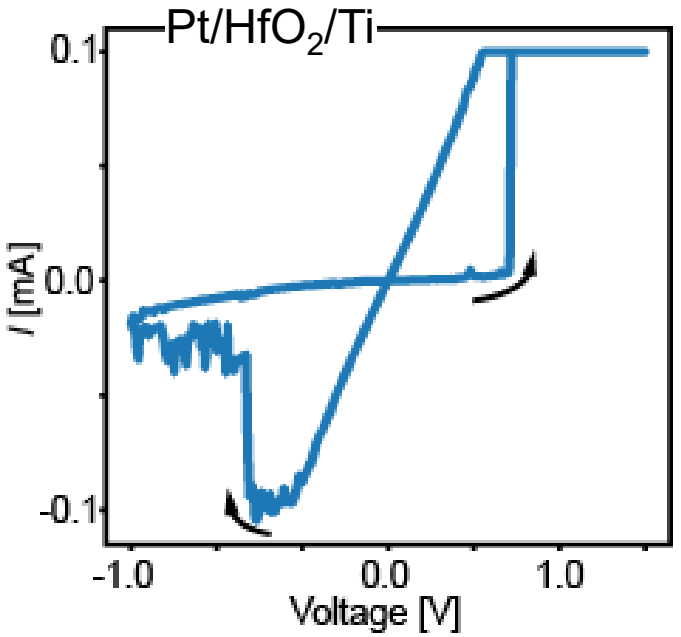

→ How do these materials differ?

C. Funck, S. Menzel, *ACS Appl. Electron.,* vol. 3, 3674-3692, (2021)

Oxygen Vacancy Defects in Oxides

C. Linderälv, P. Erhart et al.,
J. Phys. Chem. Lett., vol. 9, no. 1, 222-228

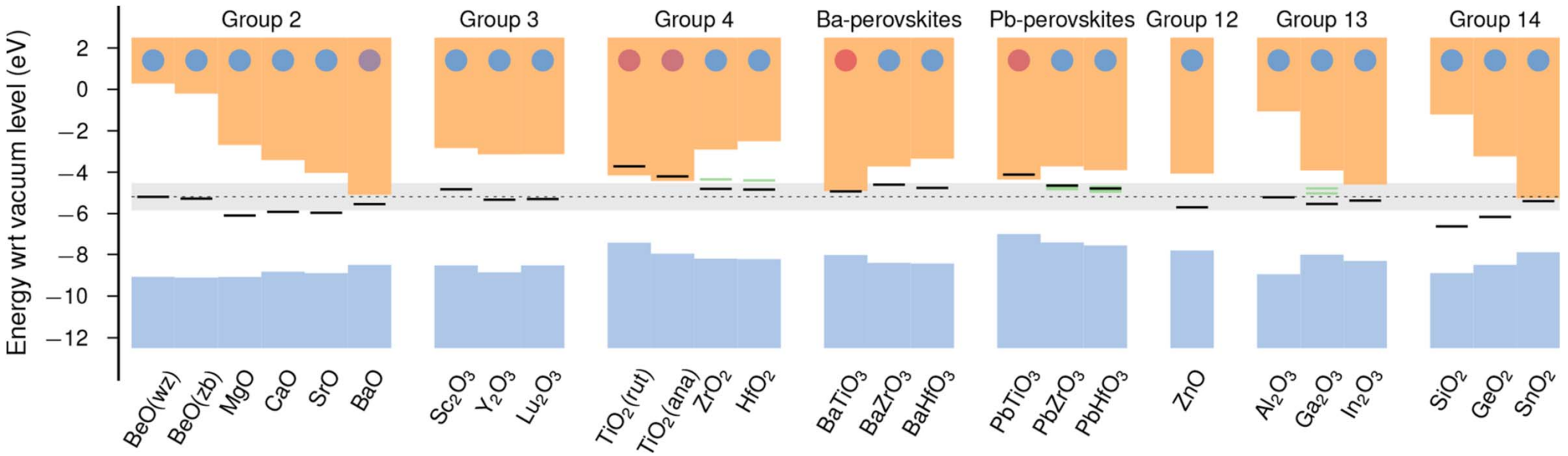

→ Type 1: shallow defect states and delocalized electrons

→ Type 2: deep defect states and localized electrons

Experimental Data Pt/$SrTiO_3$

I-V-T of multilevel states

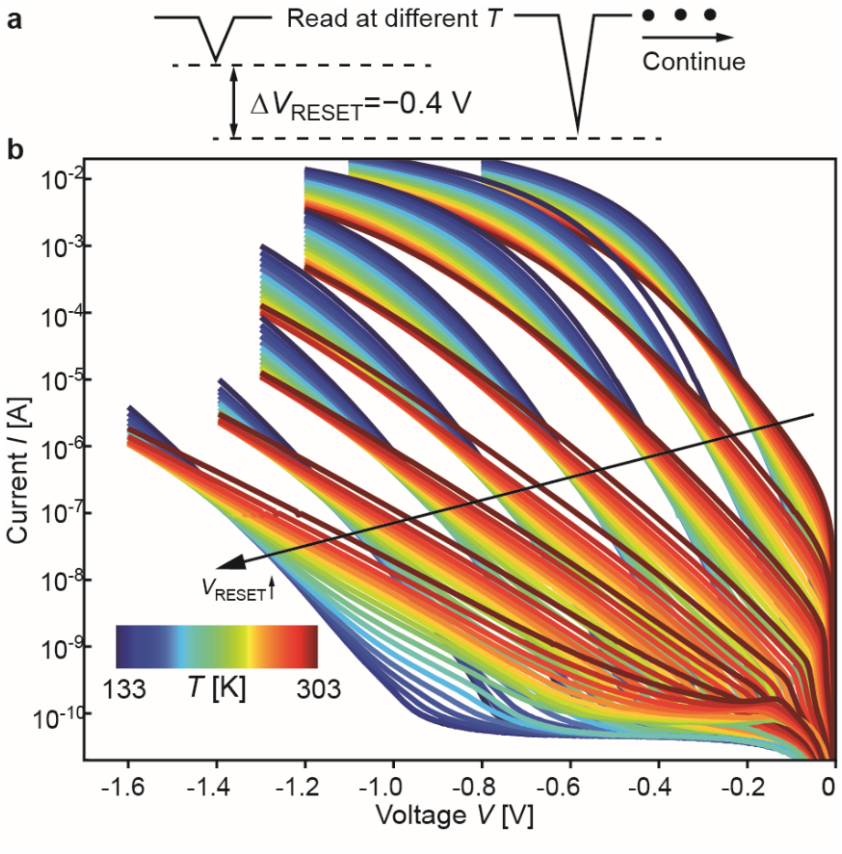

→ Change of *T*-dependence

C. Funck, S. Menzel et al.,
Phys. Rev. B, vol. 102, 035307, (2020)

I-V-T of LRS state

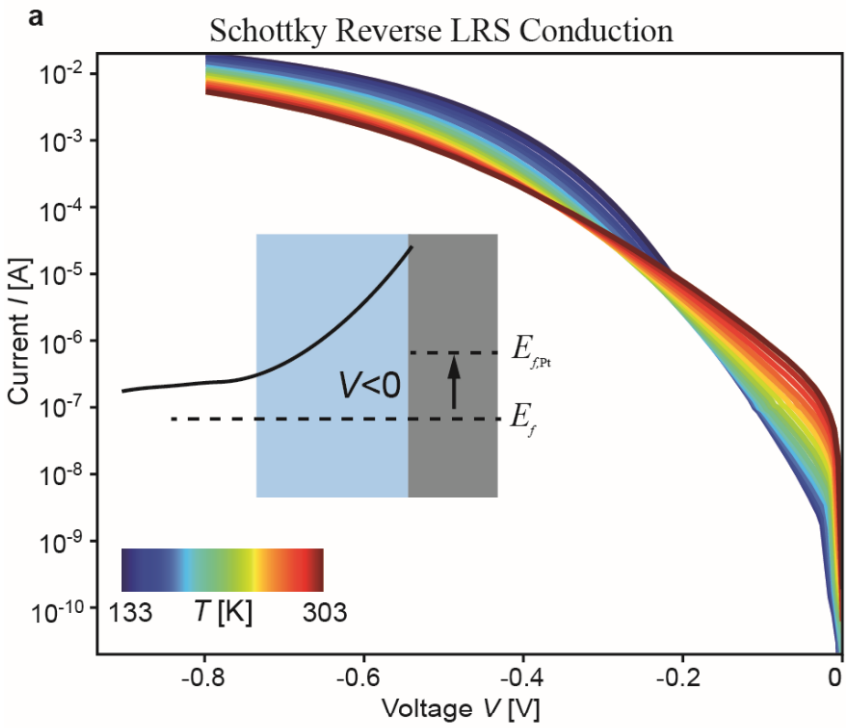

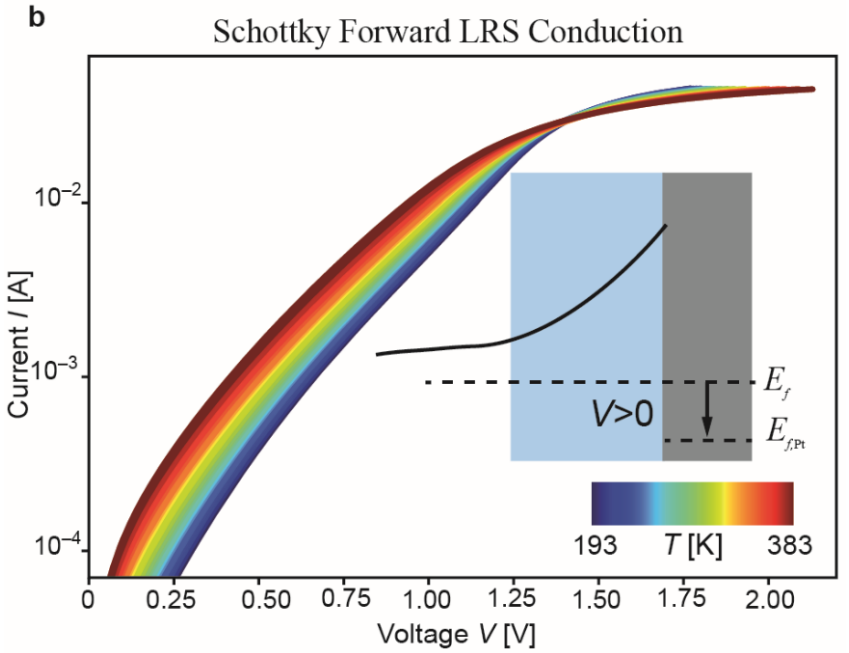

DFT-Nonequilibrium Green's Function (NEGF) Formalism

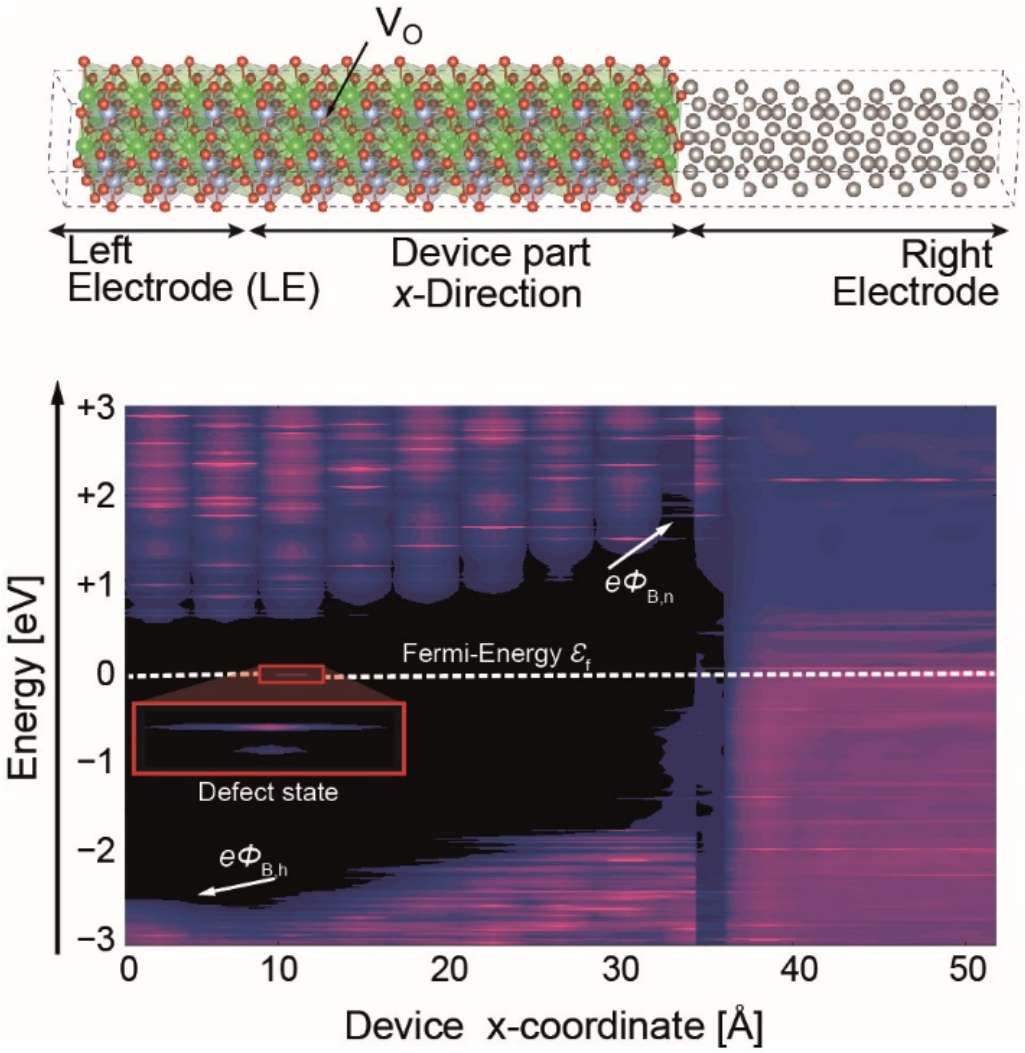

2×2×9 [100] $SrTiO_3$ supercell
2×2×4 [100] Pt supercell

↓ DFT PBE-GGA

Local density of states (LDOS)

DFT calculation details:

Code: ATK 2015
Exchange correlation: PBE

k-point Sampling for electrodes (3x3x100)

Local atomic basis set.

C. Funck, A. Marchewka, S. Menzel et al., *Adv. Electron. Mater.*, vol. 4, no. 7, 1800062, (2018)

DFT-Nonequilibrium Green's Function (NEGF) Formalism

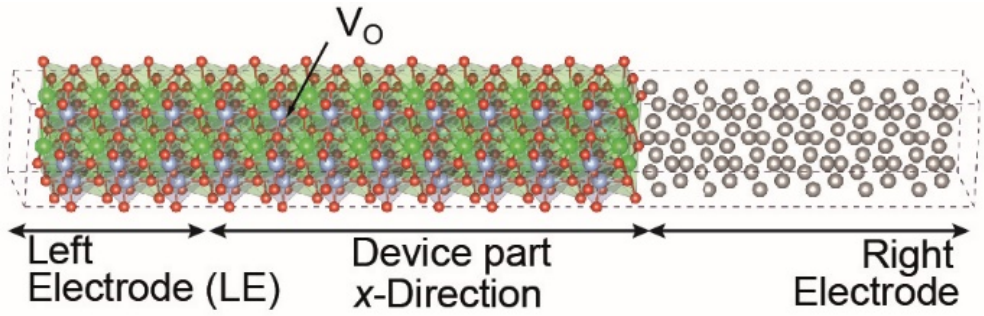

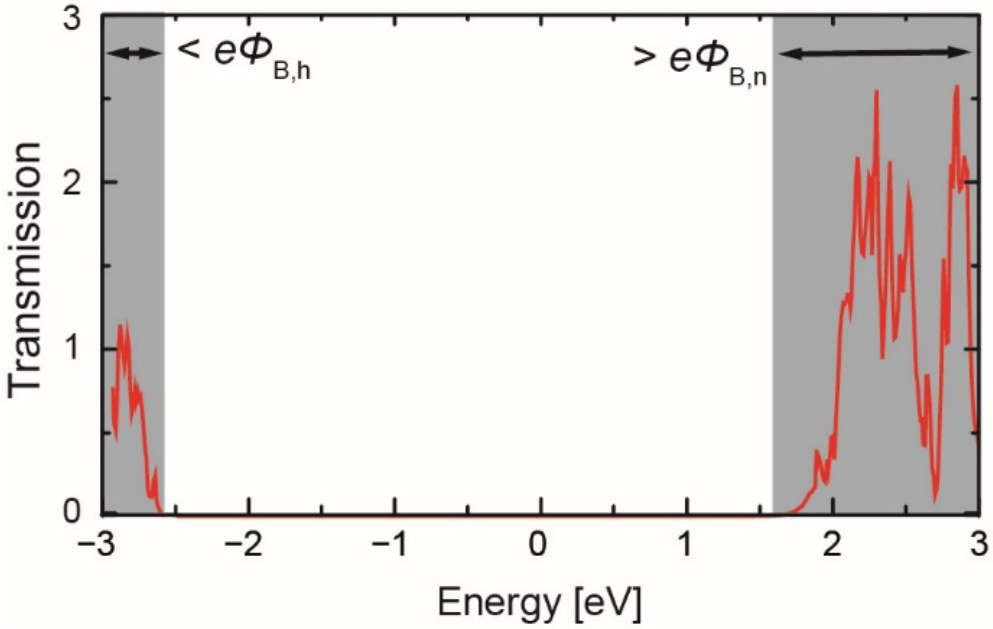

C. Funck, S. Menzel et al., *Adv. Electron. Mater.*, vol. 4, no. 7, 1800062, (2018)

$2\times2\times9$ [100] $SrTiO_3$ supercell
$2\times2\times4$ [100] Pt supercell

↓ DFT PBE-GGA

Local density of states (LDOS)

↓ NEGF

Transmission spectrum

↓ Different T
No phonon scattering

Current characteristics

$$I = \frac{e}{h}\int_{-\infty}^{\infty} T_R(E, \varepsilon_{LE}, \varepsilon_{RE})\left[f\left(E-\varepsilon_{LE}, T\right) - f\left(E-\varepsilon_{RE}, T\right)\right] dE\,,$$

Spectral Current Analysis in Reverse Direction

Continuum

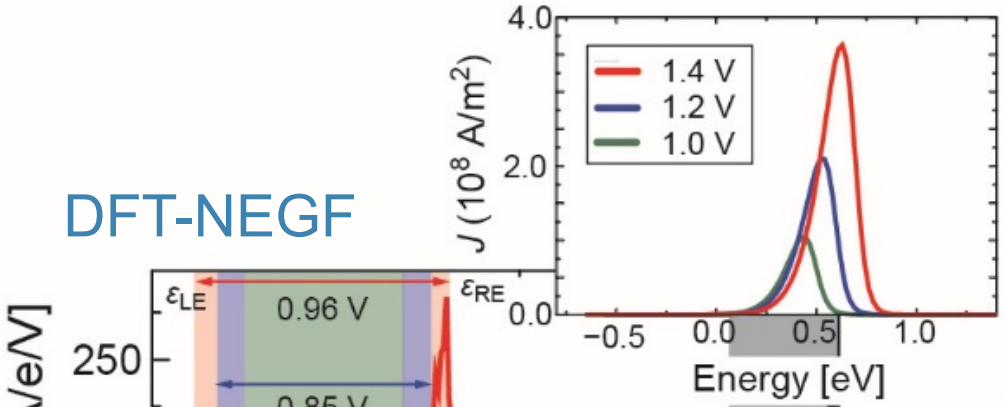

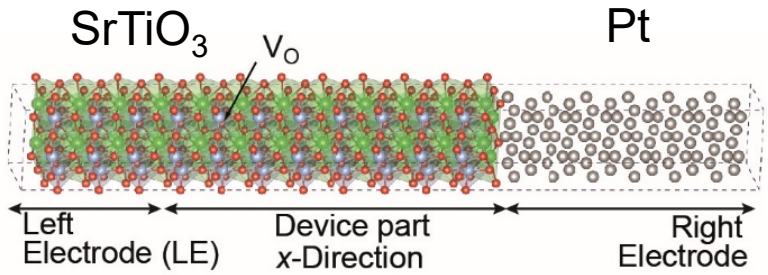

DFT-NEGF

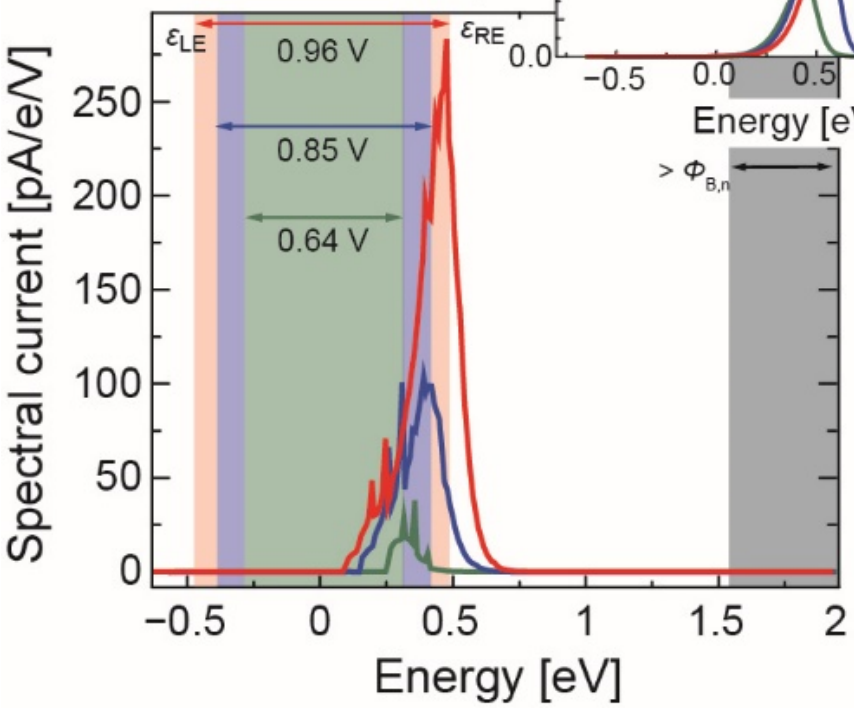

Transmission spectra

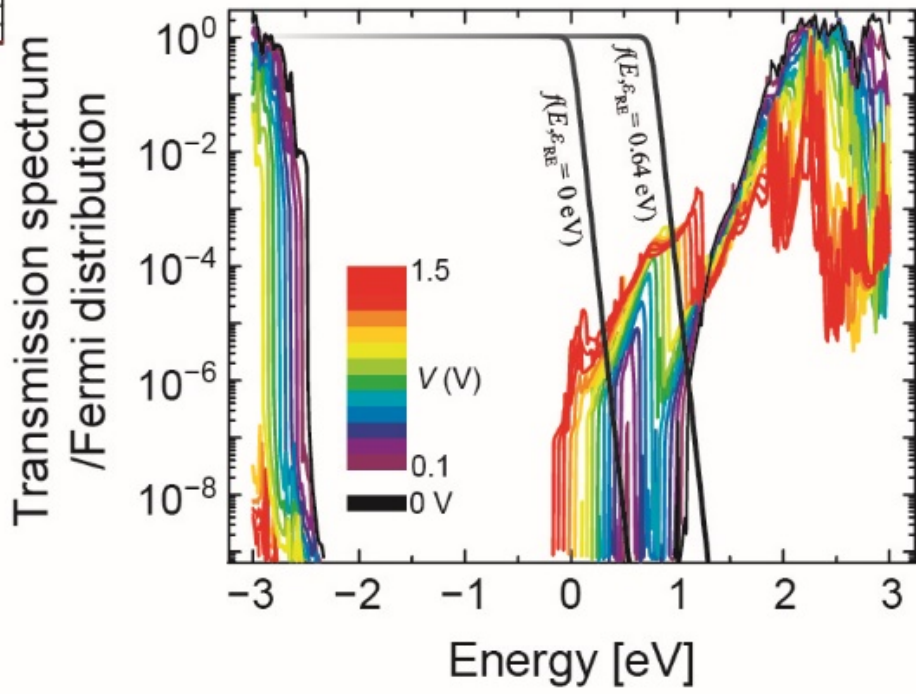

→ Spectral current reveals strong tunneling contribution

C. Funck, A. Marchewka, S. Menzel et al., *Adv. Electron. Mater.*, vol. 4, no. 7, 1800062, (2018)

Analysis of the Voltage Dependence

Low voltage regime

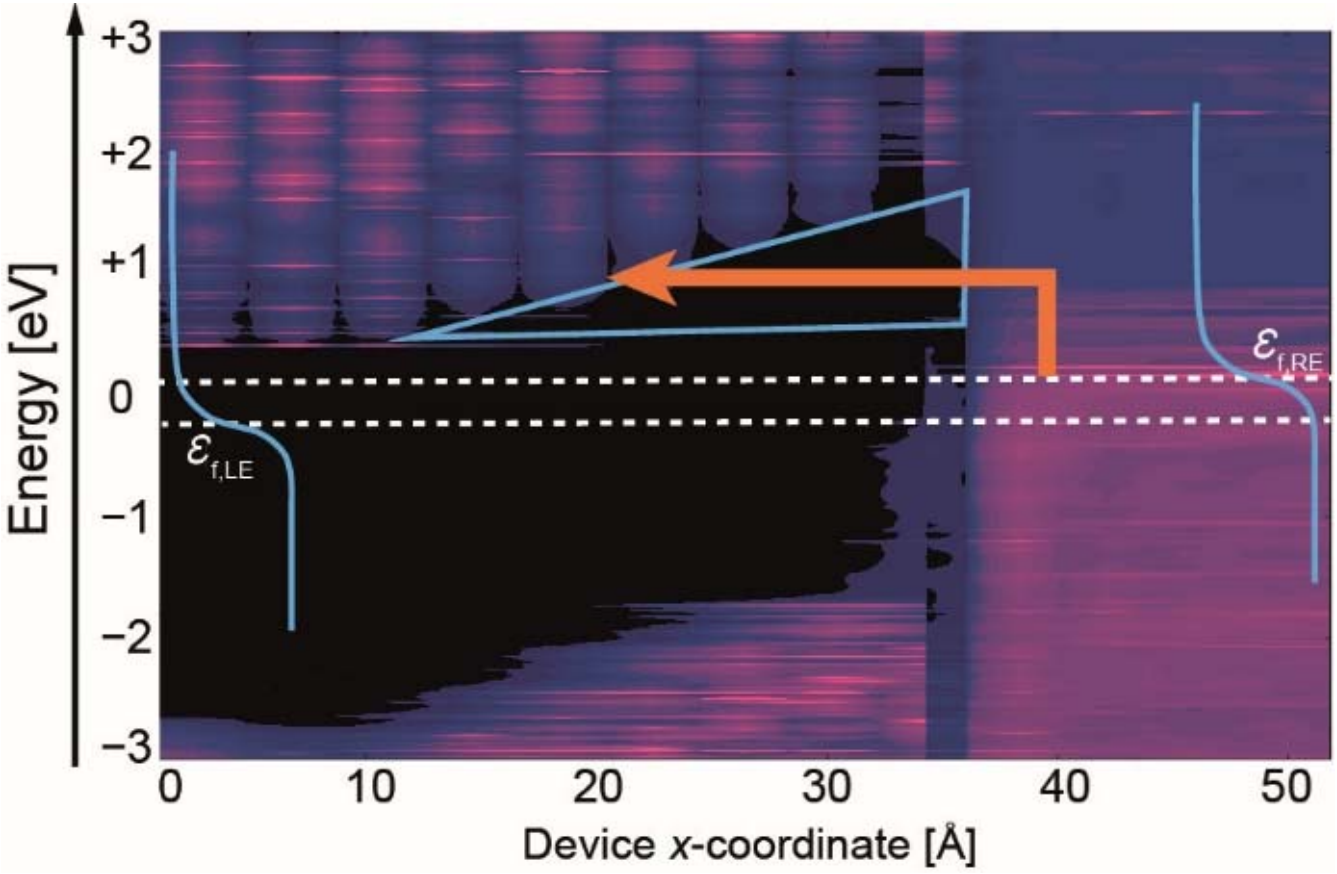

→ Only thermally excited electrons can tunnel (Boltzmann approximation valid)
→ Current increases with *T*

C. Funck, A. Marchewka, S. Menzel et al., *Adv. Electron. Mater.*, vol. 4, no. 7, 1800062, (2018)

Analysis of the Voltage Dependence

Intersection voltage V_I

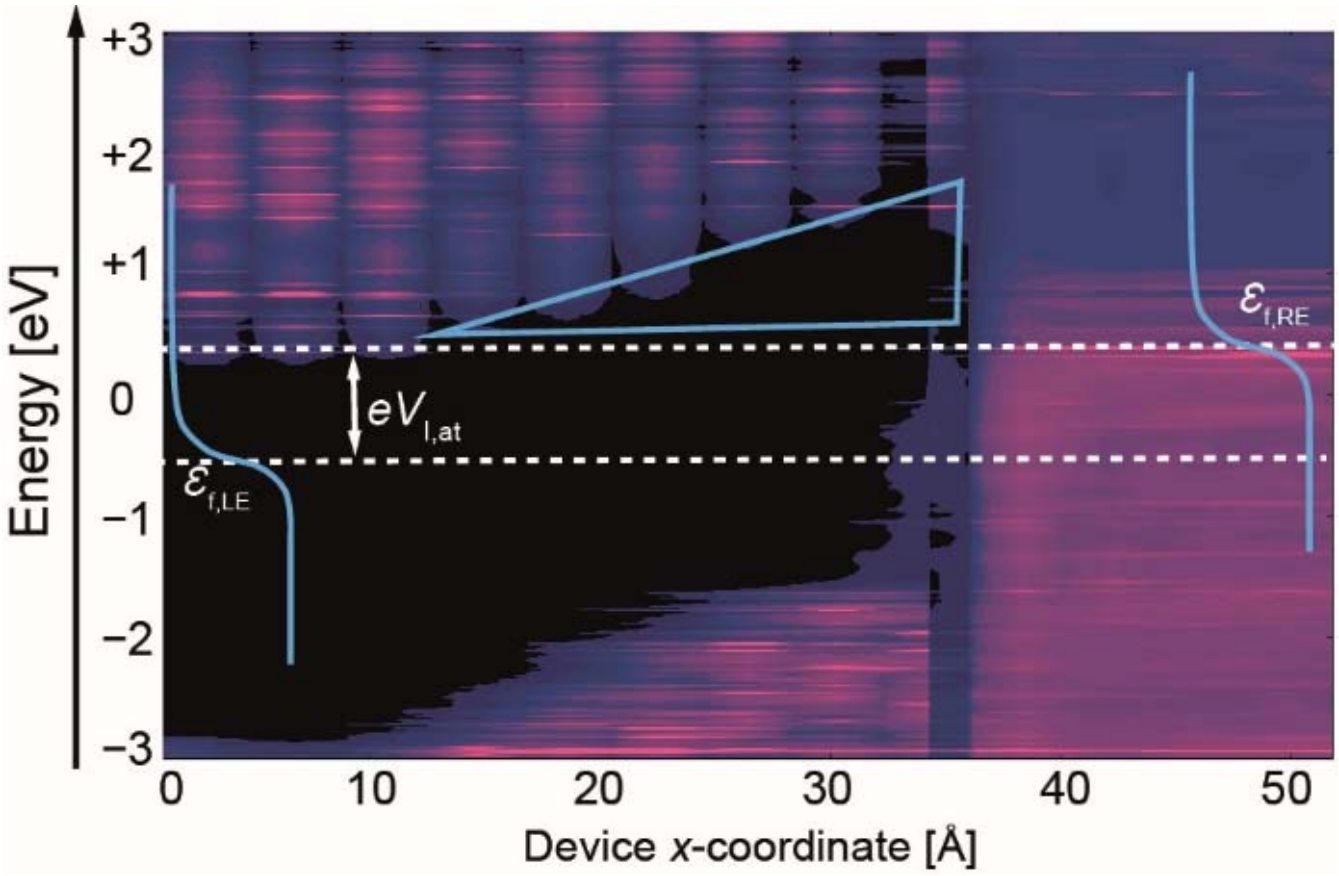

→ RE Fermi level and maximum of spectral current coincide
→ Boltzmann approximation invalid

C. Funck, A. Marchewka, S. Menzel et al., *Adv. Electron. Mater.*, vol. 4, no. 7, 1800062, (2018)

Analysis of the Voltage Dependence

High voltage regime

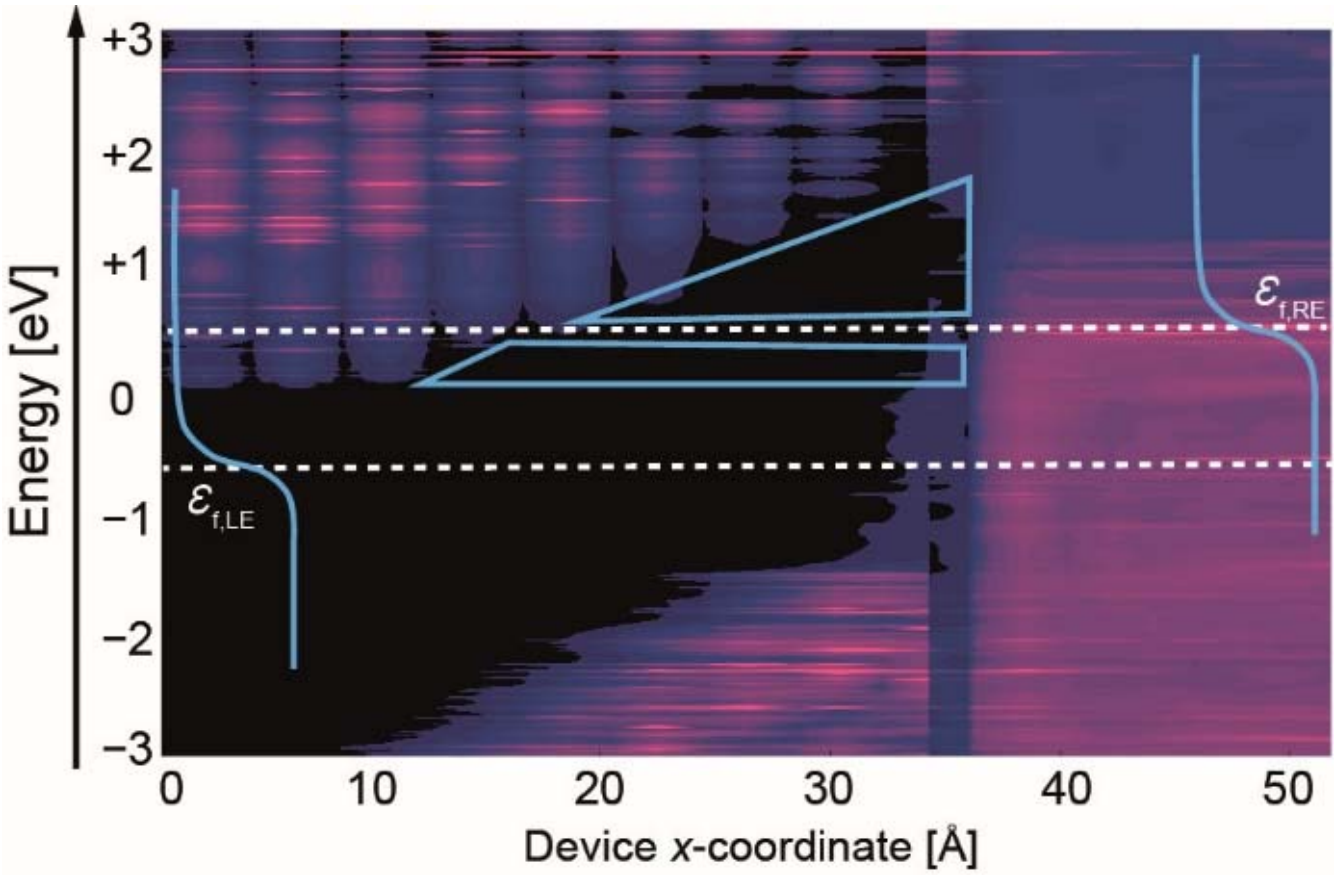

→ All electrons tunnel (no *T*-dep by tunneling)

→ *T*-dependence due to phonon scattering

C. Funck, A. Marchewka, S. Menzel et al., *Adv. Electron. Mater.*, vol. 4, no. 7, 1800062, (2018)

Summary of Type I Conduction

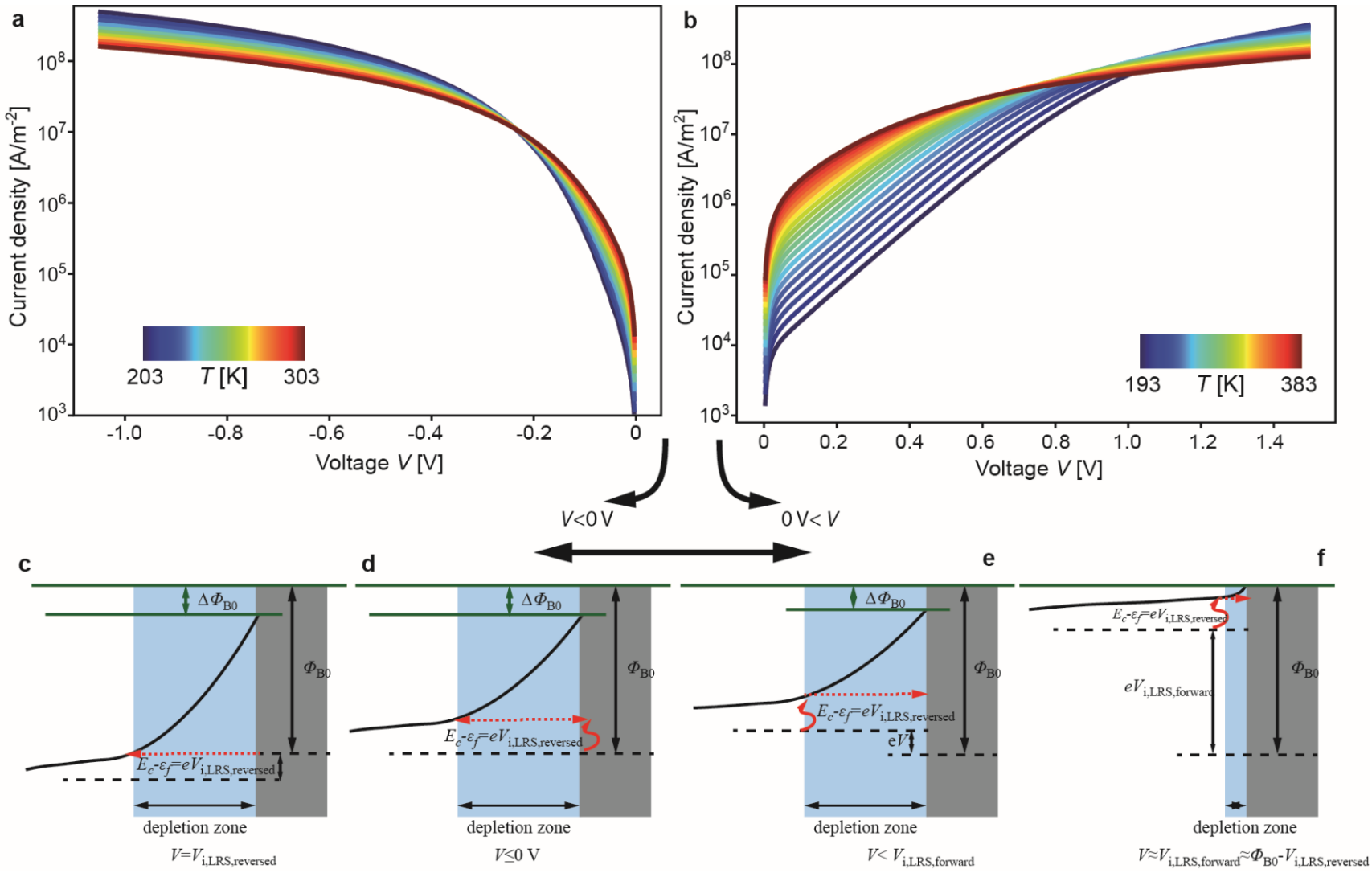

C. Funck, S. Menzel et al., *Phys. Rev. B*, vol. 102, 035307, (2020)

DFT-NEGF Simulation of the HRS

C. Funck, S. Menzel, *ACS Appl. Electron.*, vol. 3, 3674-3692, (2021)

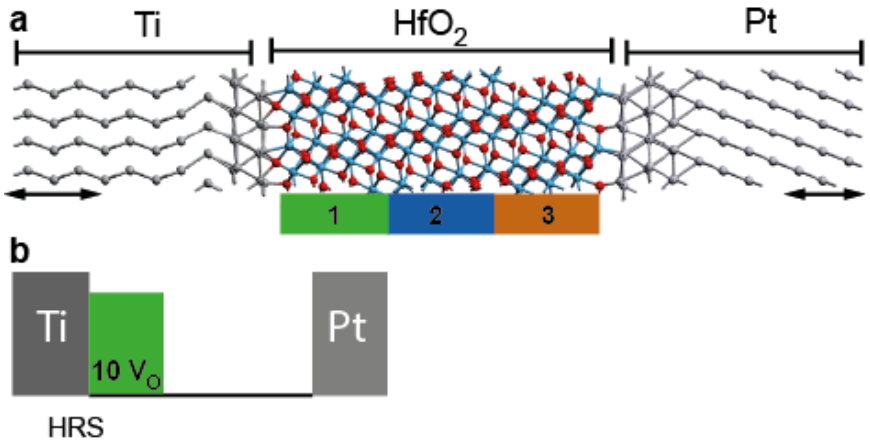

LRS

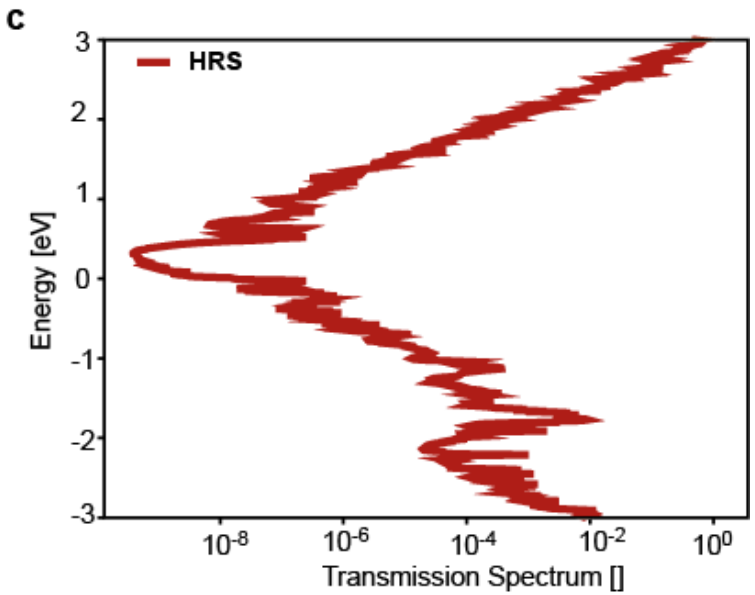

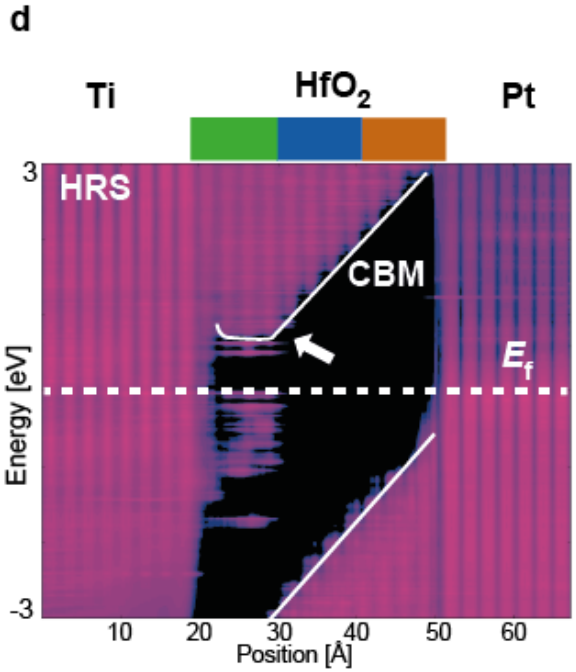

DFT-NEGF Simulation of an IRS

C. Funck, S. Menzel, *ACS Appl. Electron.*, vol. 3, 3674-3692, (2021)

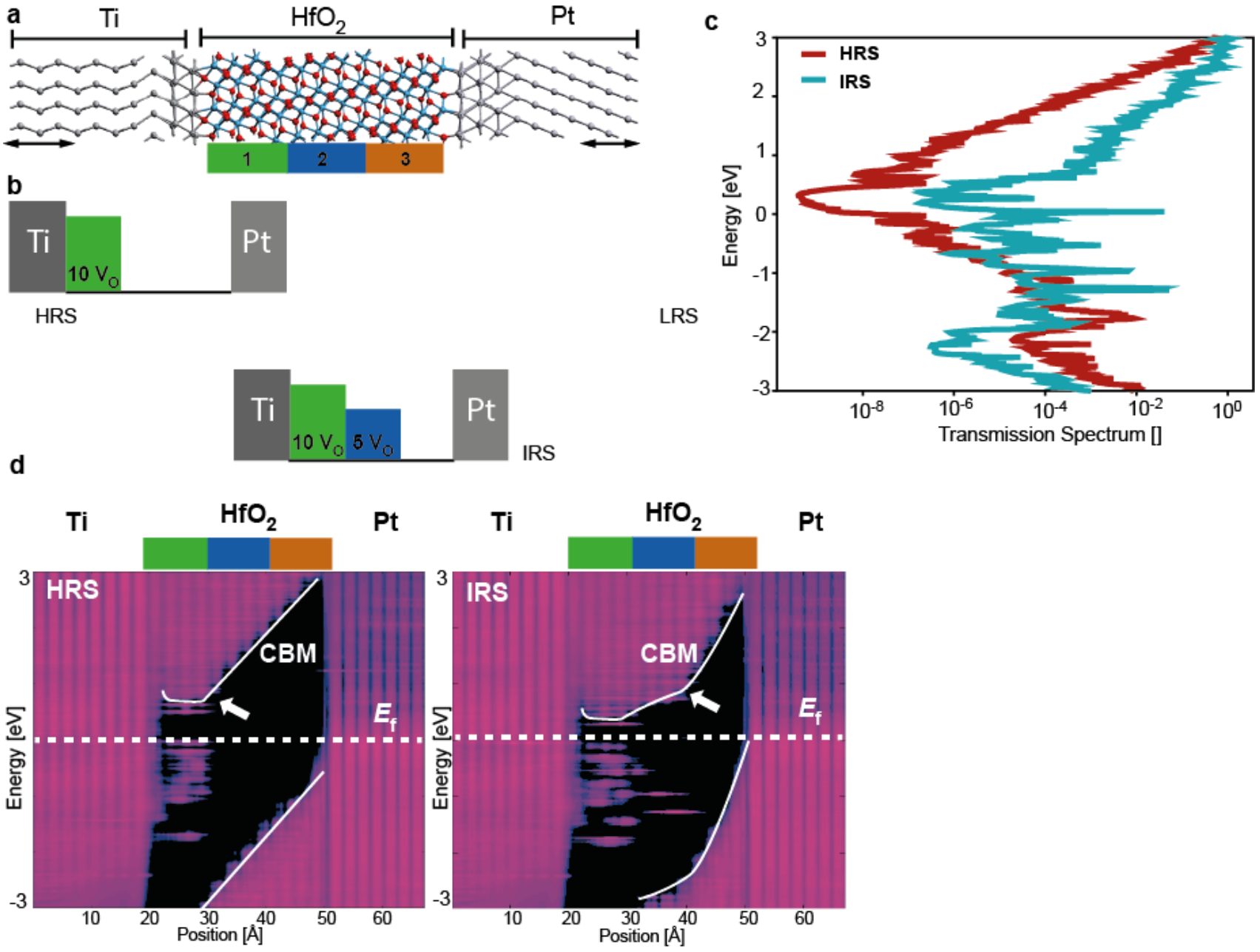

DFT-NEGF Simulation of the LRS

C. Funck, S. Menzel, *ACS Appl. Electron.*, vol. 3, 3674-3692, (2021)

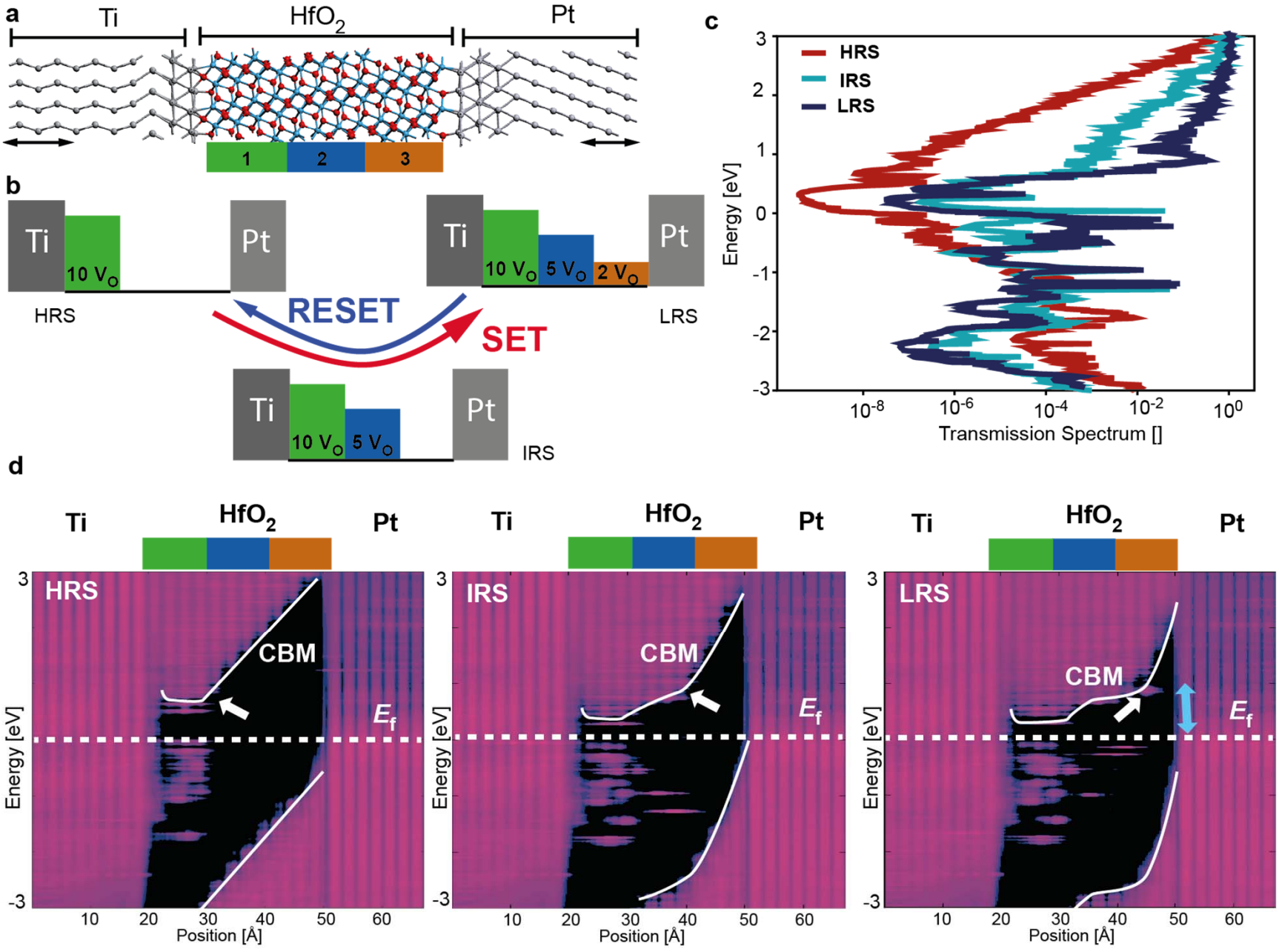

General Switching Mechanism

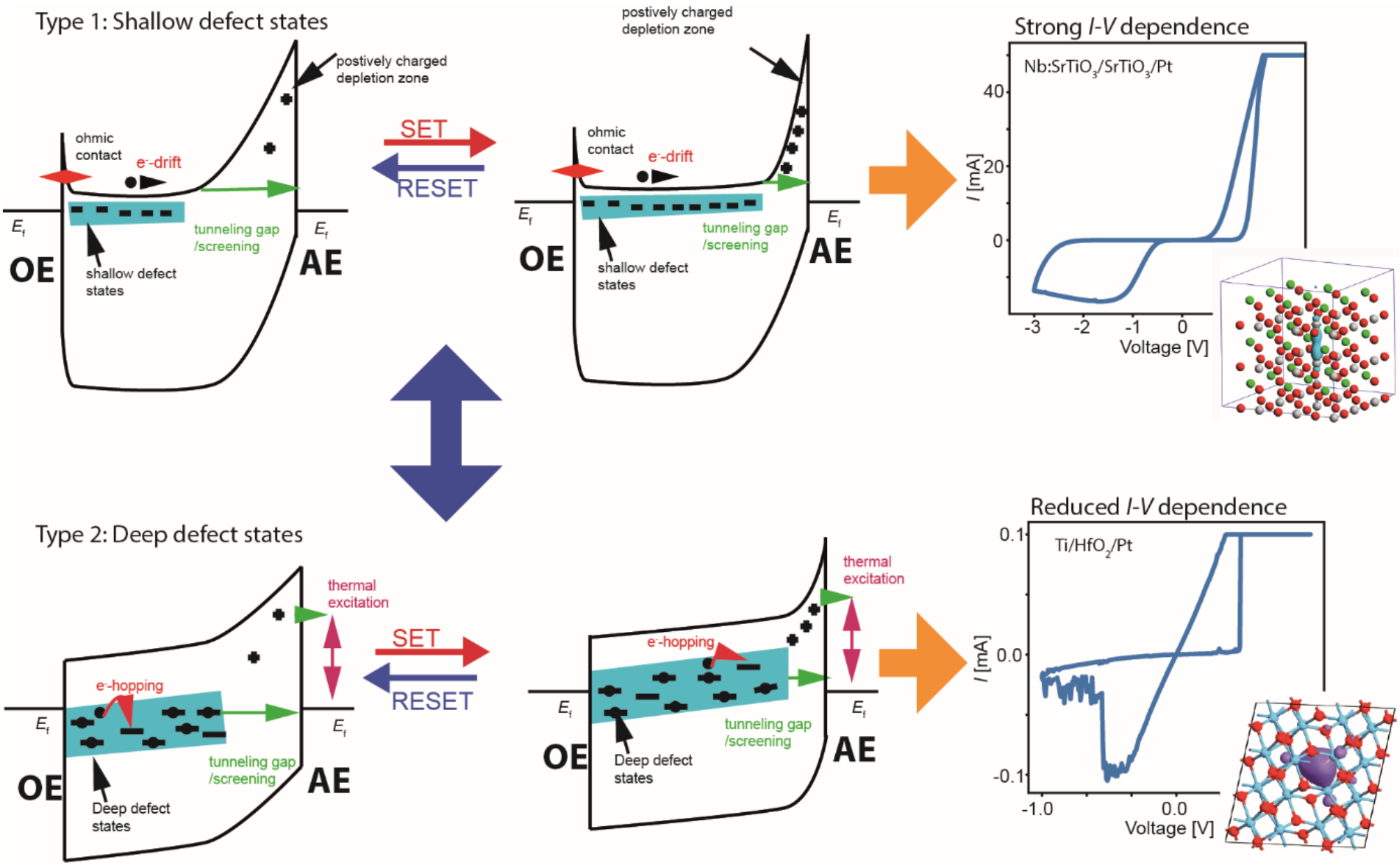

R. Dittman, S. Menzel, R. Waser, Advances in Physics, DOI: 10.1080/00018732.2022.2084006

Outline

- Motivation
- Electronic Transport in VCM Cells: A DFT-NEGF study
- **Switching Variability of VCM Cells: Kinetic Monte Carlo Modeling**
- Switching Dynamics of VCM Cells: Continuum Modeling
- Towards Circuit Simulations: VCM Compact Models (JART)
- Array Level Modeling
- Summary & Conclusion

KMC Model I: Electronic Model

Simulation geometry

- Oxide cube of 5 nm x 5 nm x 5 nm
- Possible defect sites every 0.5 nm (= a)
- Active (AE) and ohmic electrode (OE)

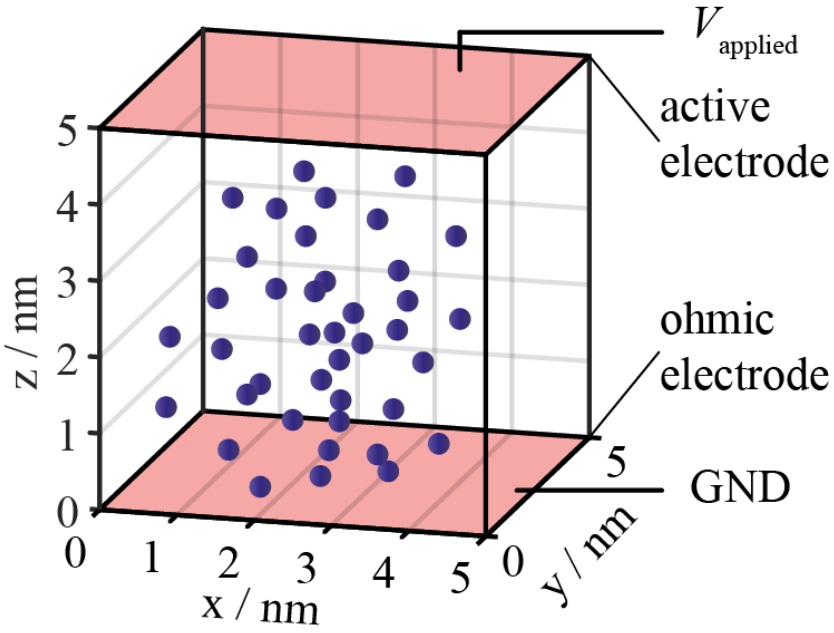

Defects

- Oxygen vacancies $V_O^{\cdot\cdot}$
- Reduced cations close to $V_O^{\cdot\cdot}$ act as electron traps

Conduction mechanism (Type II)

- Trap assisted tunnneling
- (1) e^- tunneling between electrode & traps
- (2) e^- hopping between traps
- At high defect densities band conduction

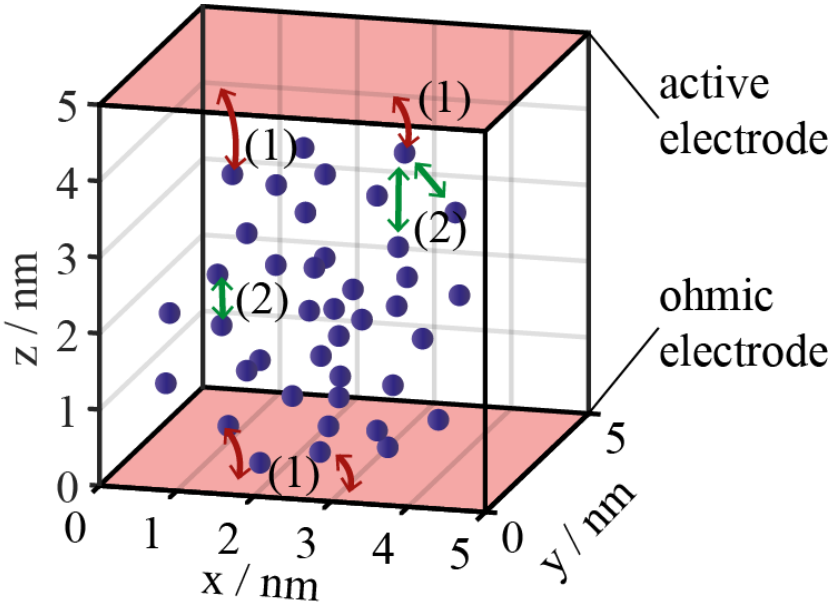

KMC Model II: Ionic Model

Dynamic model

- Joule heating
- Oxygen exchange reaction at BE
- $V_O^{\cdot\cdot}$ hopping

$$\Gamma_{G,R,D} = \nu_0 \exp\left(-\frac{\Delta W_{G,R,D} - \alpha_i z E}{k_B T}\right)$$

- Weighted random selection of process
- Time increment

$$\Delta t = -\frac{\ln(\Gamma_i)}{\Gamma_{total}}$$

Simulation flow

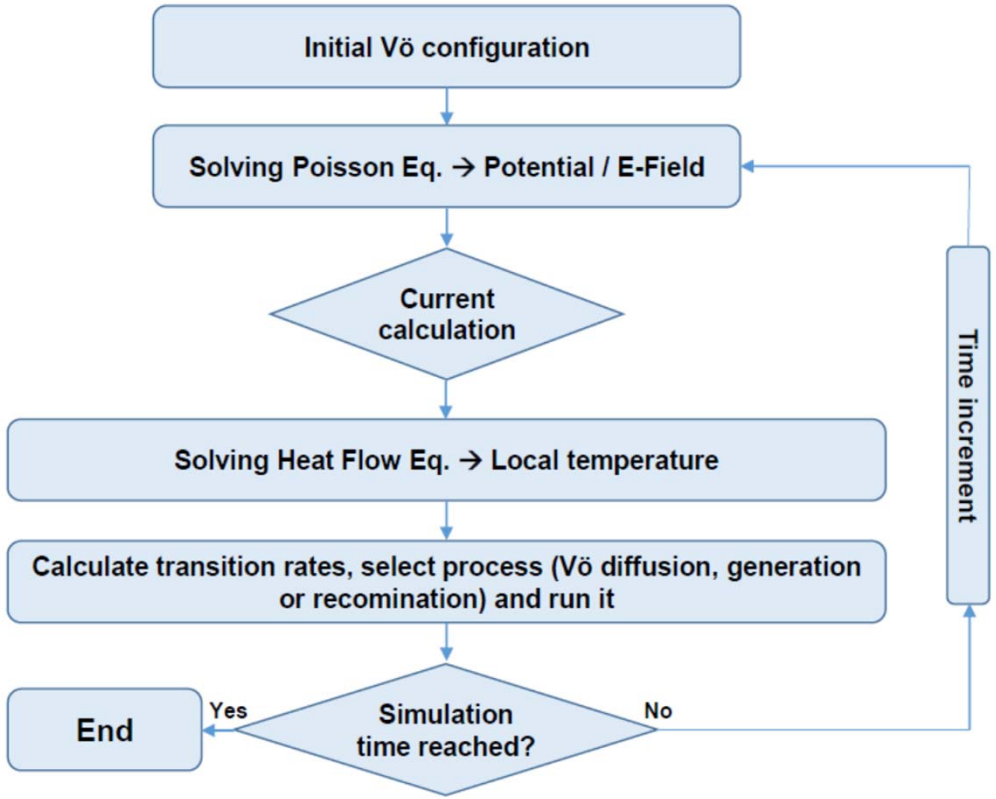

E. Abbaspour, S. Menzel, C. Jungemann et. al, *IEEE Trans. Nanotechnology,* vol. 17, no. 6, pp. 1181-1188 (2018)

E. Abbaspour, S. Menzel, C. Jungemann, *Journal of Computational Electronics,* vol. 19, pp. 1426-1432 (2020)

Origin of the Switching Variability: Stochasticity

Simulation of 100 *I-V* cycles

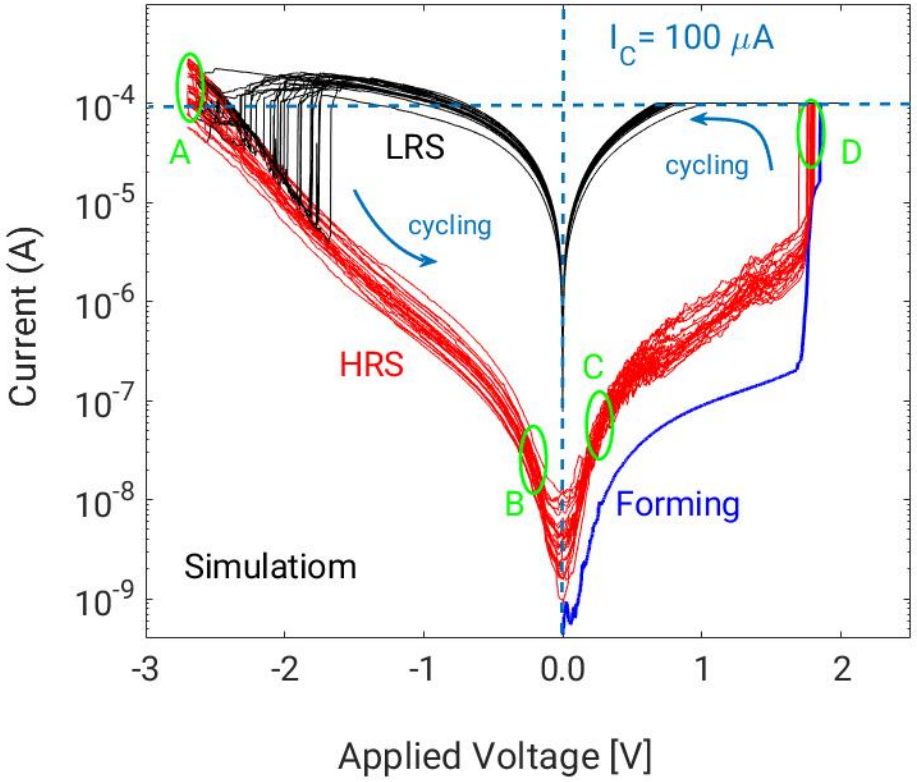

Filament evolution

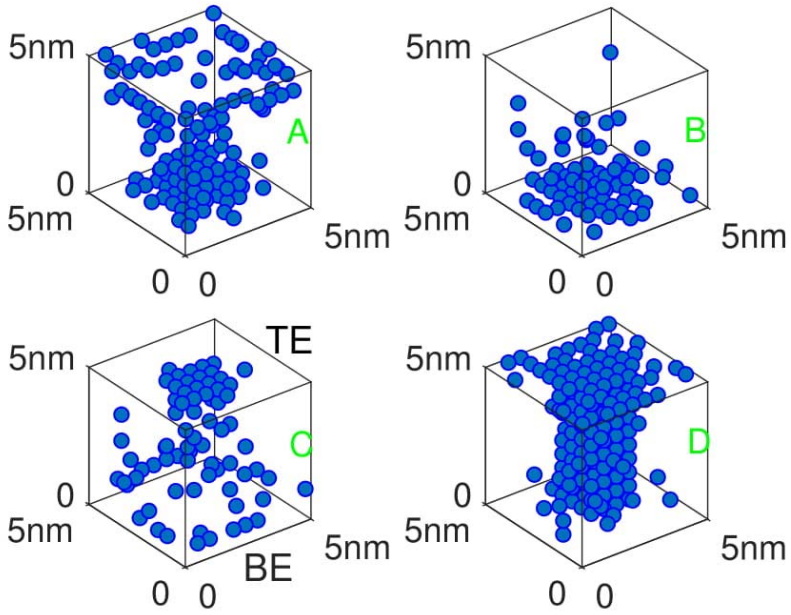

→ Typical SET/RESET switching obtained

E. Abbaspour, S. Menzel, C. Jungemann et. al,
IEEE Trans. Nanotechnology, vol. 17, no. 6, pp. 1181-1188 (2018)

Origin of the Switching Variability: Stochasticity II

SET switching probability

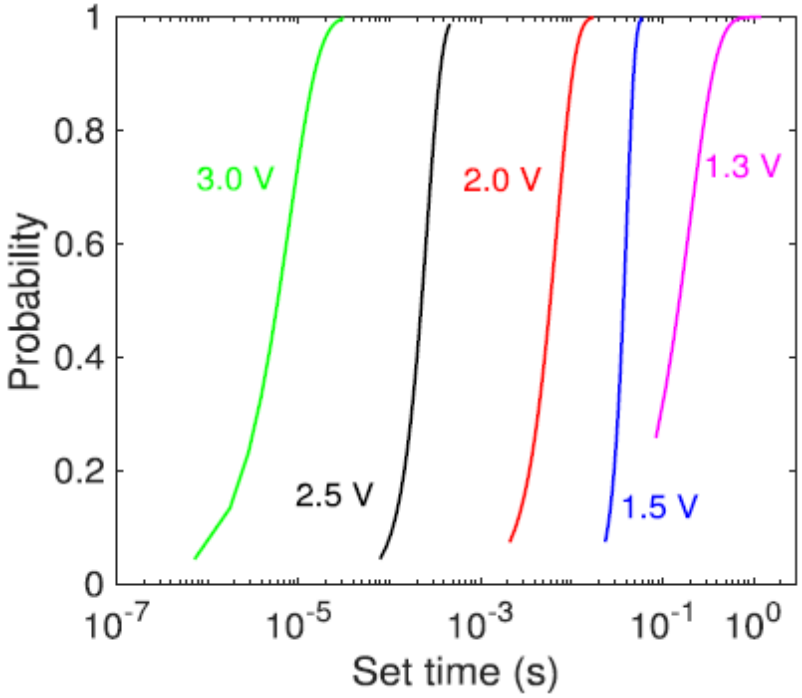

HRS/LRS distributions

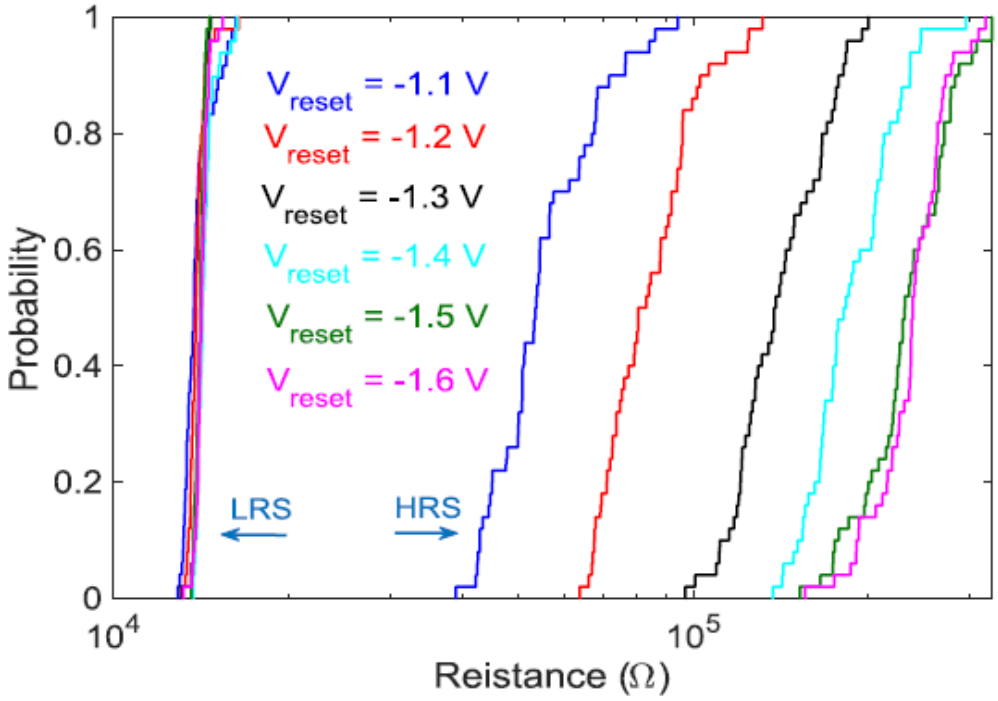

→ Distributions tighter than in experiment

→ Stochasticity is not sufficent to explain variability

E. Abbaspour, S. Menzel, C. Jungemann, *Journal of Computational Electronics,* vol. 19, pp. 1426-1432 (2020)

Relation between Read Instability & Retention

Retention (shifts & tilts)

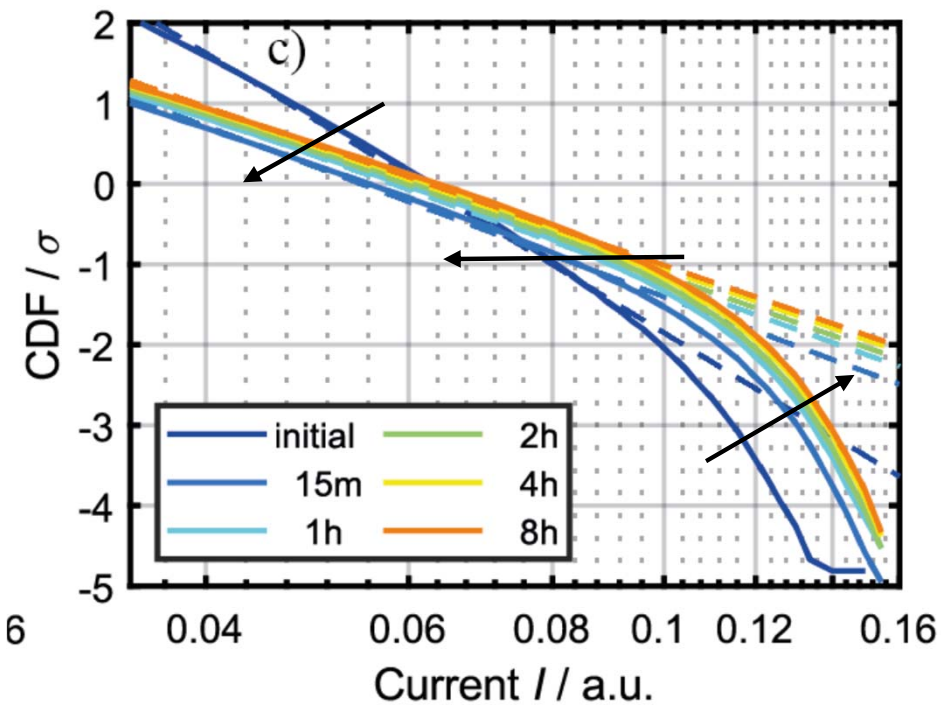

S. Wiefels, S. Menzel et al.,
IEEE IMW (2020)

Read instability

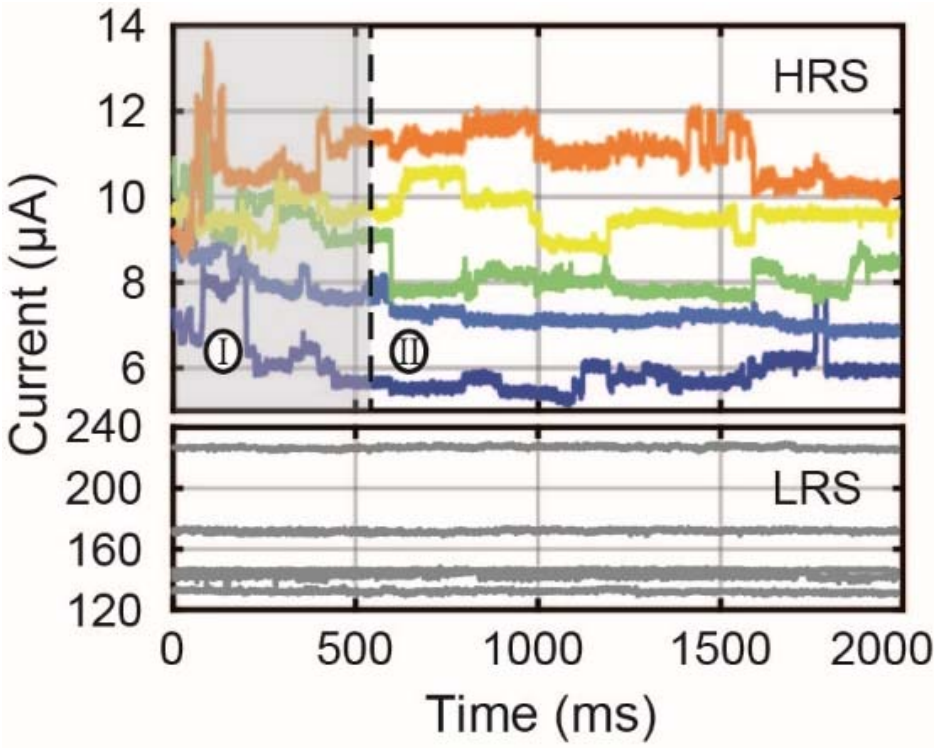

S. Wiefels, S. Menzel et al., *IEEE T-ED*,
vol. 67, no. 10, pp. 4208-4215 (2020)

→ Both processes depends on ionic motion,
but occur on different timescales !?

Physical Model Idea

MD Simulation of ion transport in amorphous HfO_2

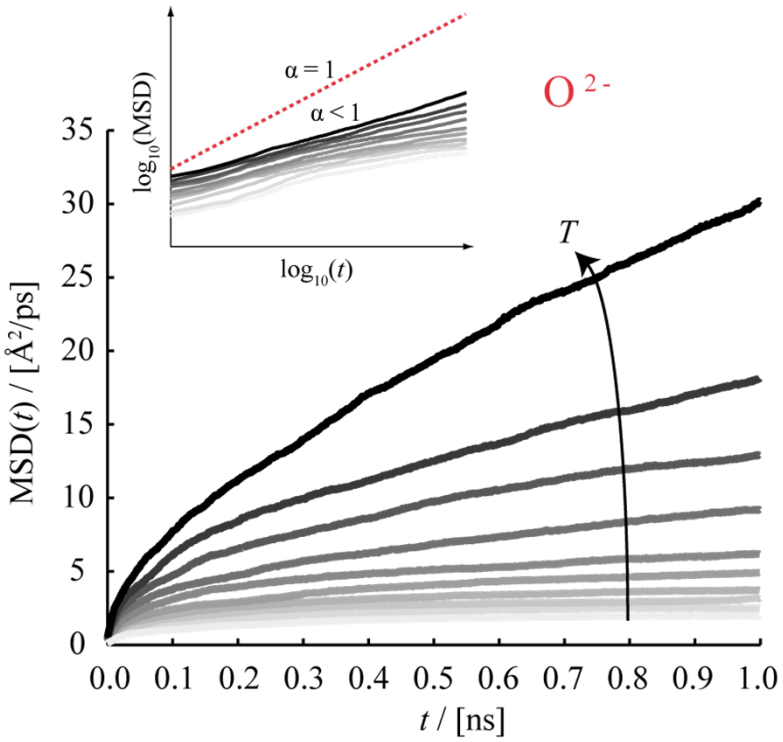

M. Schie, R. de Souza et al., *J. Chem. Phys.*, vol. 9, no. 146, 94508 (2017)

Sub-diffusive transport

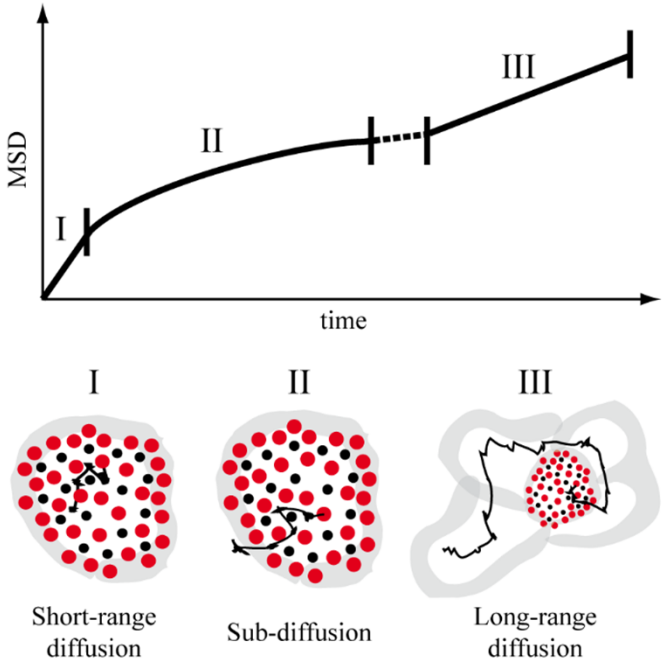

→ Different diffusive regions

KMC Multi-Domain Model I

Model

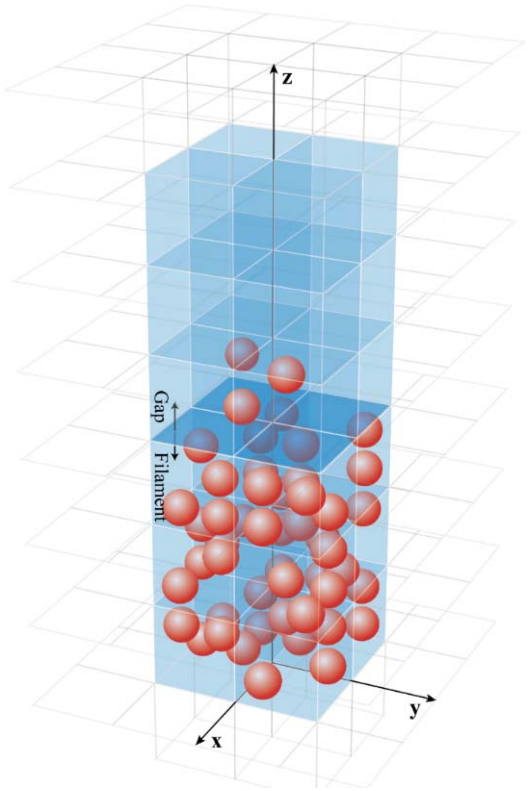

Read Instability

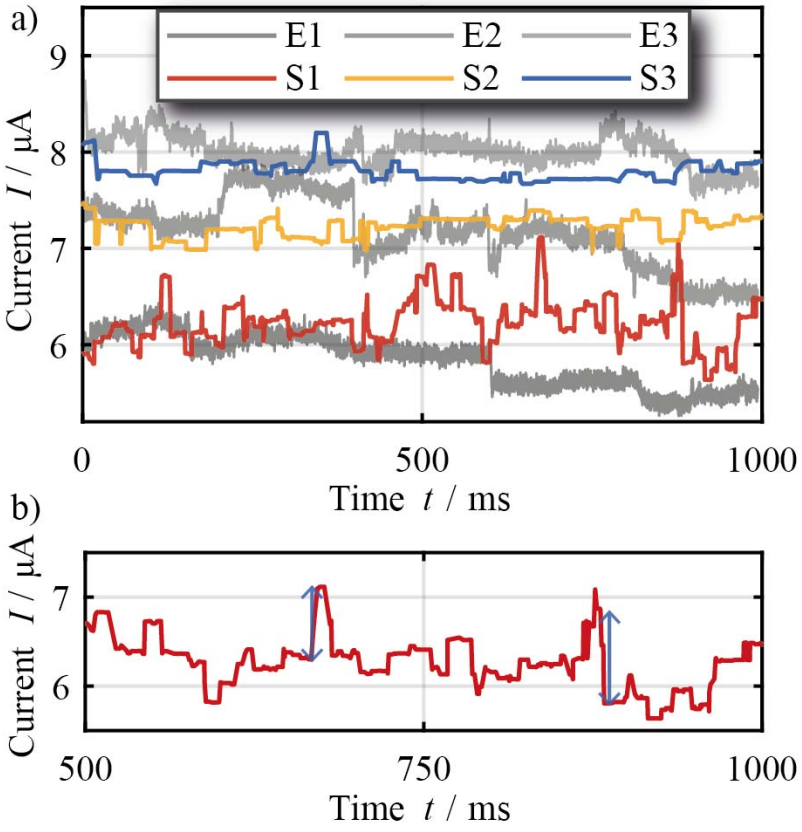

→ Read instability due to jumps in the boxes

N. Kopperberg, S. Menzel *et al.*, ACS Appl. Materials & Interfaces, 13, 48, 58066-58075, 2021

KMC Multi-Domain Model II

Tilting of the distribution

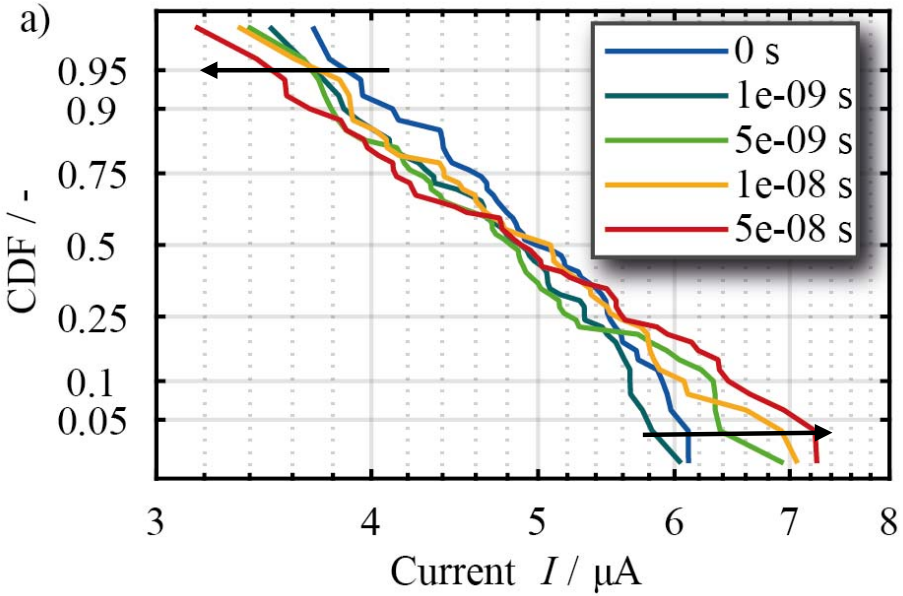

Shift of the distribution

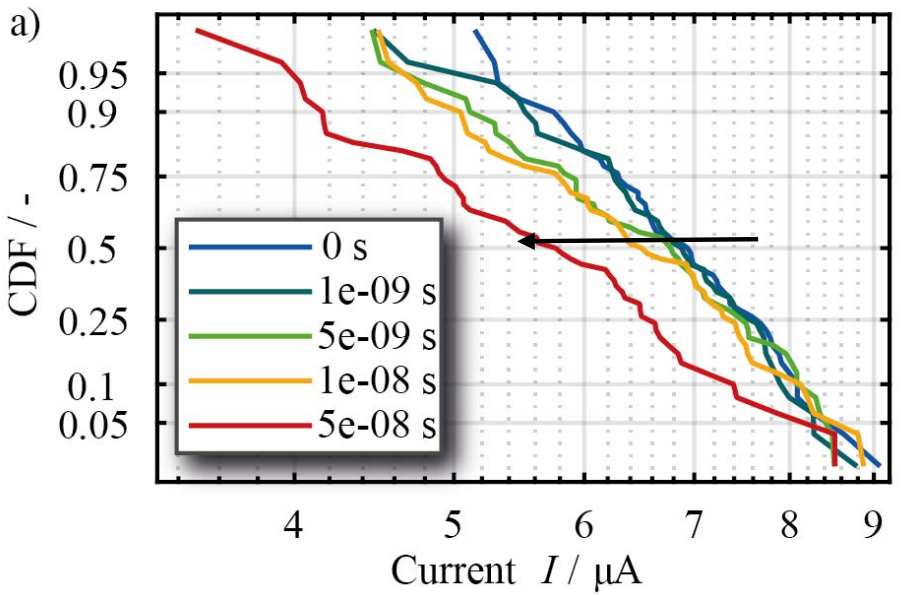

→ Retention due to jumps out of the boxes
→ depends on initial state

N. Kopperberg, S. Menzel *et al.*, ACS Appl. Materials & Interfaces, 13, 48, 58066-58075, 2021

Outline

- Motivation
- Electronic Transport in VCM Cells: A DFT-NEGF study
- Switching Variability of VCM Cells: Kinetic Monte Carlo Modeling
- **Switching Dynamics of VCM Cells: Continuum Modeling**
- Towards Circuit Simulations: VCM Compact Models (JART)
- Array Level Modeling
- Summary & Conclusion

VCM Continuum Model I: Equation system

Non-isothermal drift-diffusion equation for doubly charged V_O

$$\frac{\partial N_{V_O}^{2+}}{\partial t} - \nabla\left(\mu_{V_O} N_{V_O}^{2+} \nabla\psi + D_{V_O} \nabla N_{V_O}^{2+} - N_{V_O}^{2+} D_{TV_O} \nabla T\right) = -R_{V_O,2}$$

Drift-diffusion equation for electrons (Type I)

$$\nabla\left(\mu_n n \nabla\psi - D_n \nabla n + e D_{Tn} \nabla T\right) = \pm \frac{\partial j_{n,tunnel}}{\partial x}$$

Poisson equation

$$\nabla\left(\varepsilon \nabla\psi\right) = -e\left(n - N_{V_O}^{+} - 2N_{V_O}^{2+}\right)$$

Heat equation

$$-\nabla\left(k \nabla T\right) = jF$$

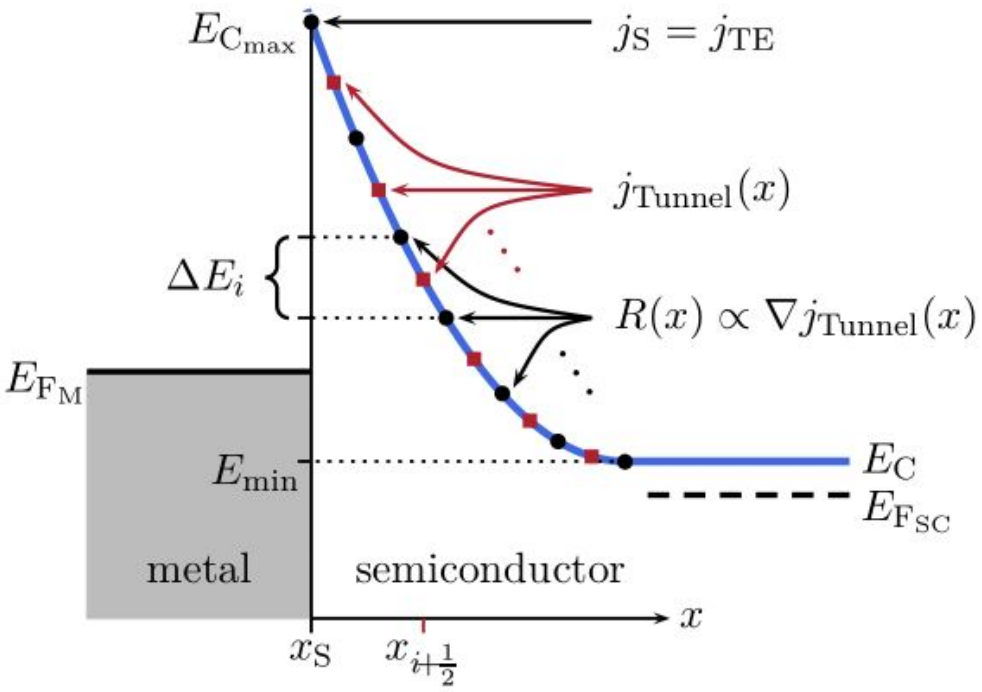

A. Marchewka, S. Menzel et al.,
Adv. Electron. Mater., 2016, vol. 2, no. 1

A. Marchewka, S. Menzel et al., SISPAD (2015)

VCM Continuum Model II: 2D Domains and Initial Conditions

Drift-diffusion equation

Heat transfer equation

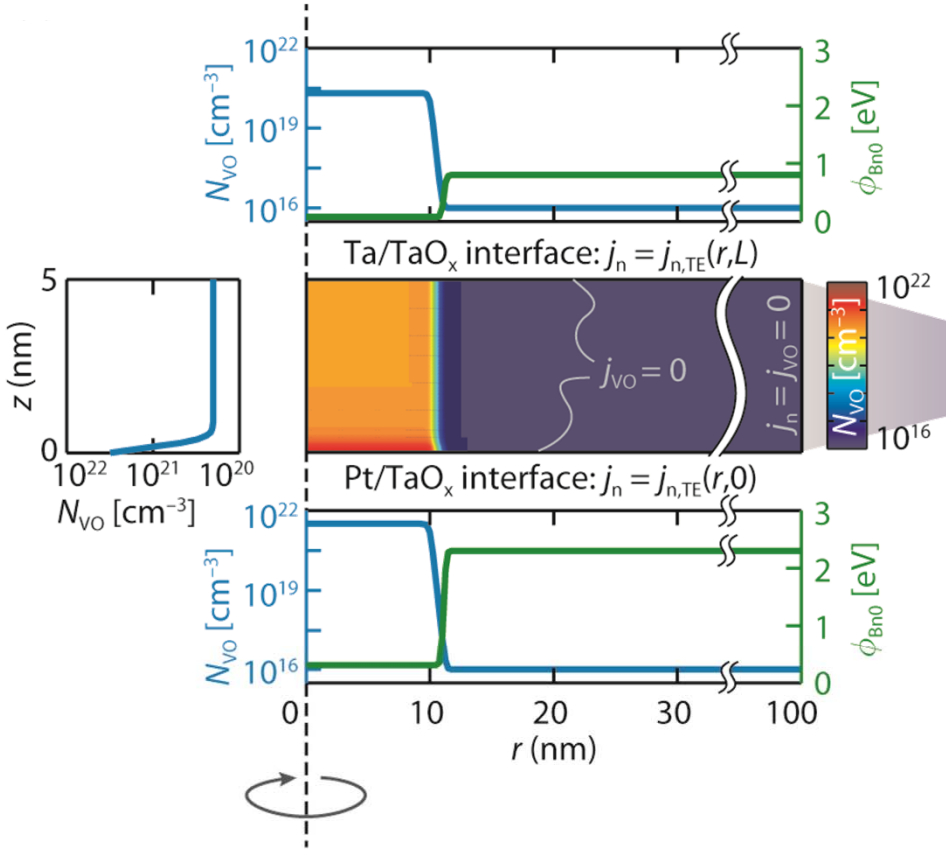

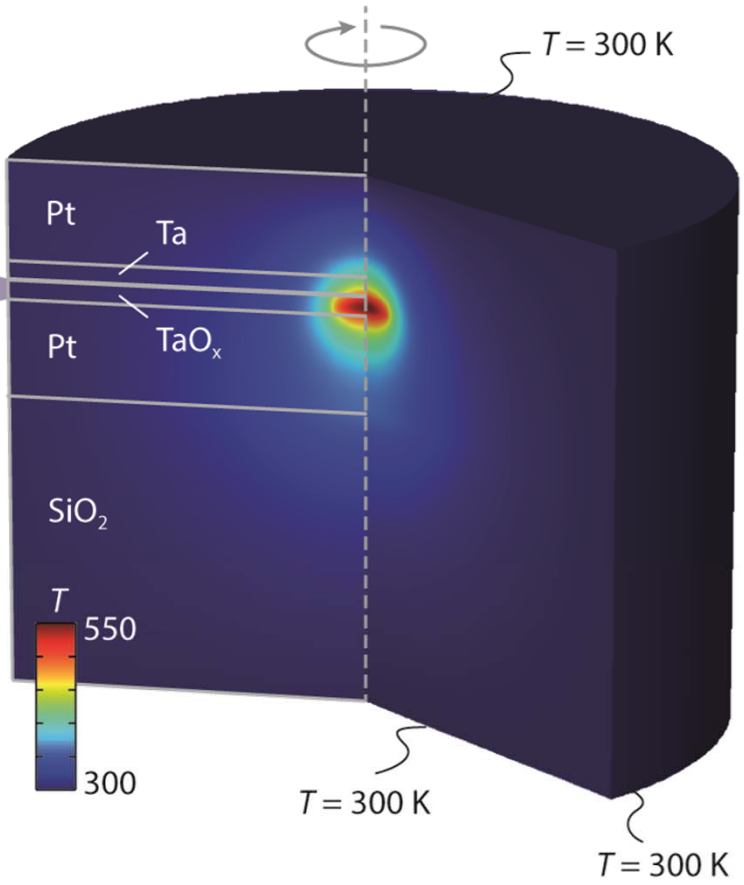

A. Marchewka, S. Menzel et al.,
Adv. Electron. Mater., vol. 2, no. 1, 1500233 (2016)

Simulated *I-V* Characteristics

A. Marchewka, S. Menzel et al.,
SISPAD 2016

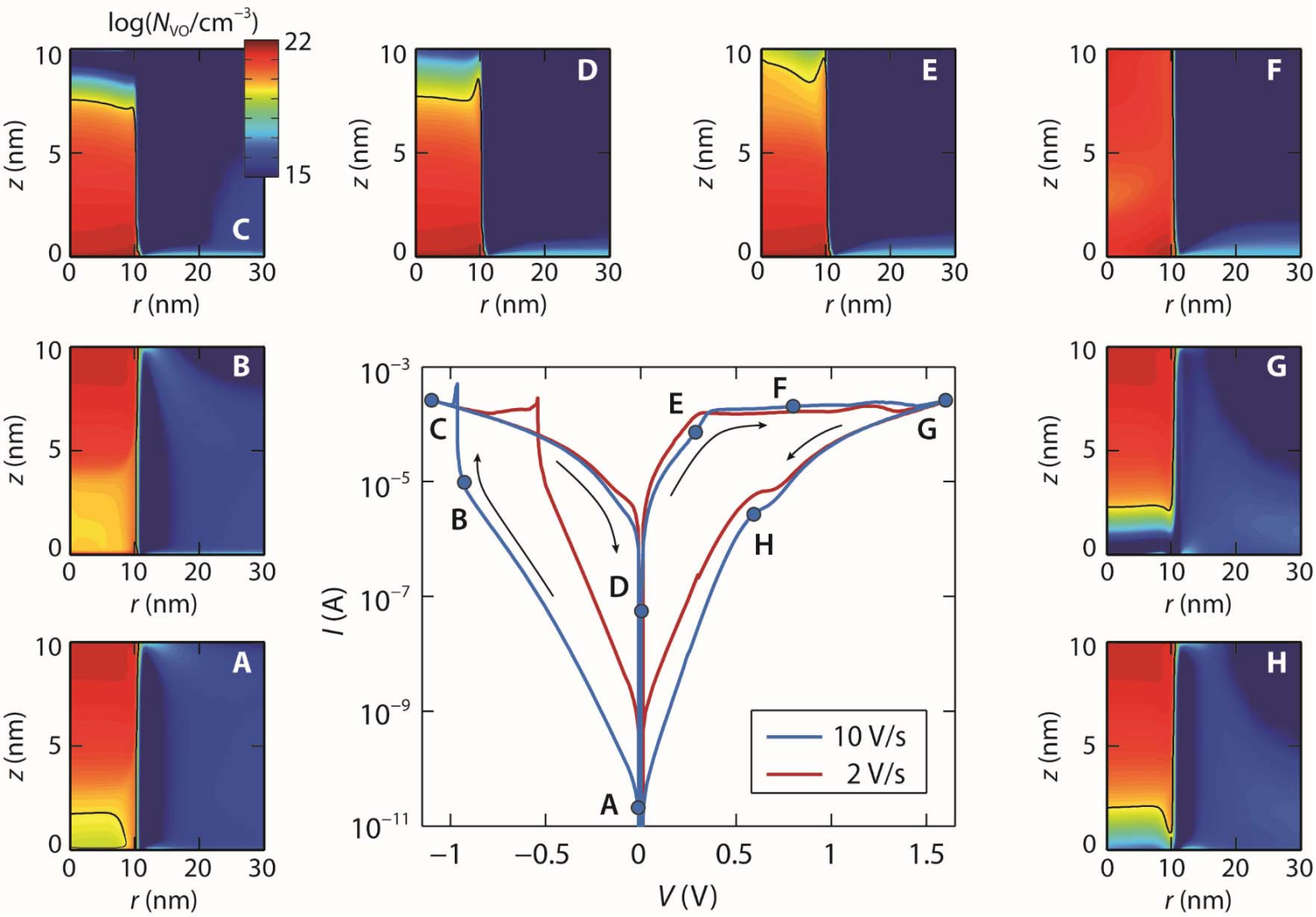

→ Bipolar c8w-switching due to asymmetric barriers
(change of concentration in front of active electrode dominant)

Continuum Modeling of SET Dynamics

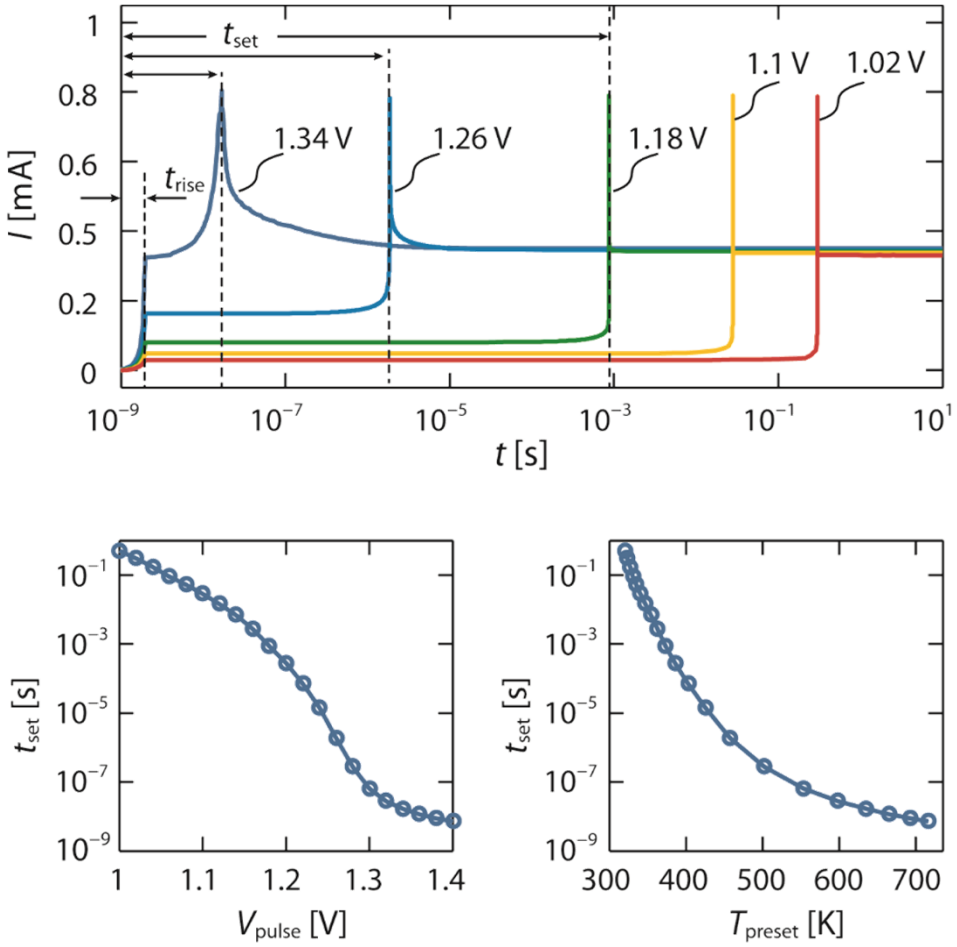

Comparison to $Pt/SrTiO_3/Ti$ cell

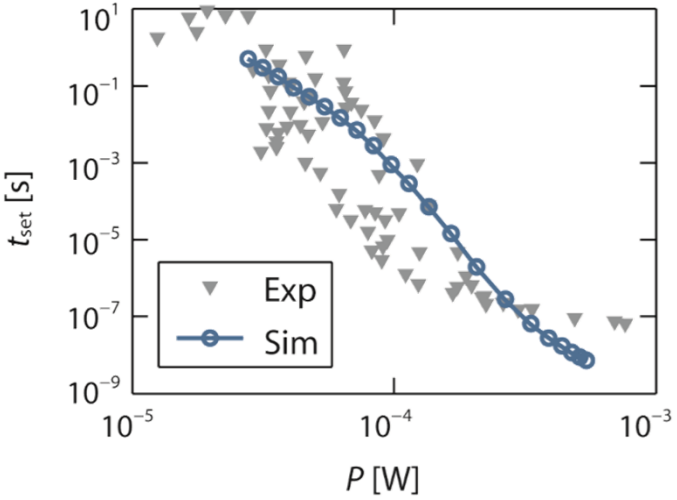

A. Marchewka, S. Menzel et al., SISPAD (2015)

→ Simulated current transients reproduce experimental behavior

→ Simulation model reproduces experimental power dependence

RESET Kinetics I: Simulation Results

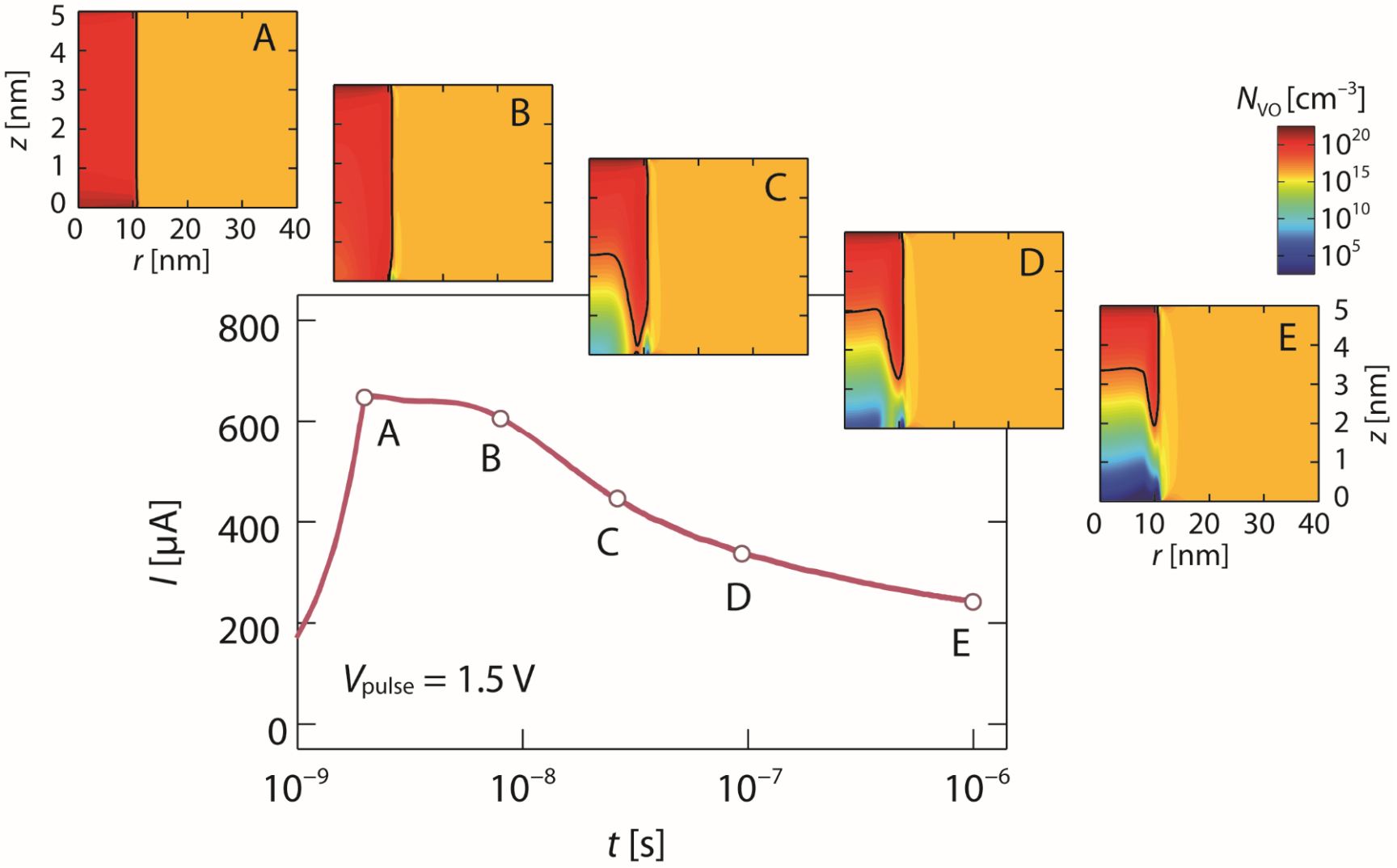

A. Marchewka, S. Menzel et al., *Adv. Electron. Mater.*, vol. 2, no. 1, 1500233 (2016)

RESET Kinetics II: Simulation Results

Transient currents

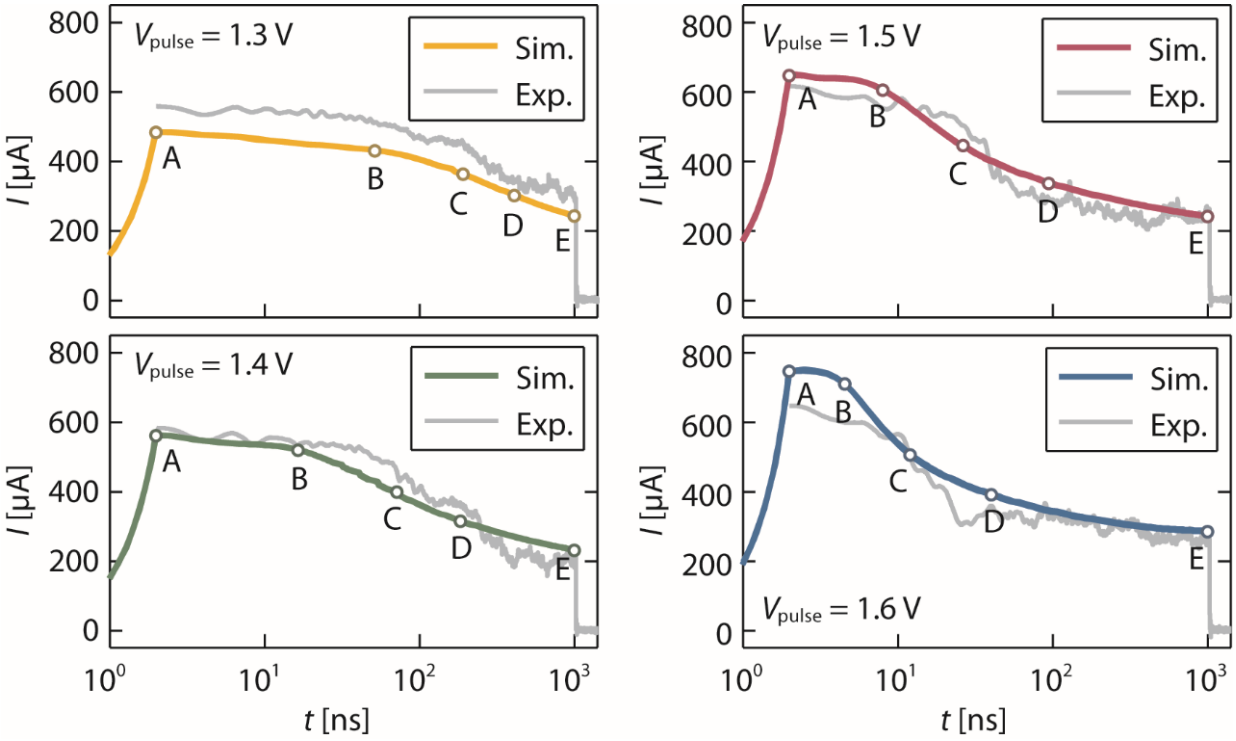

Decay times

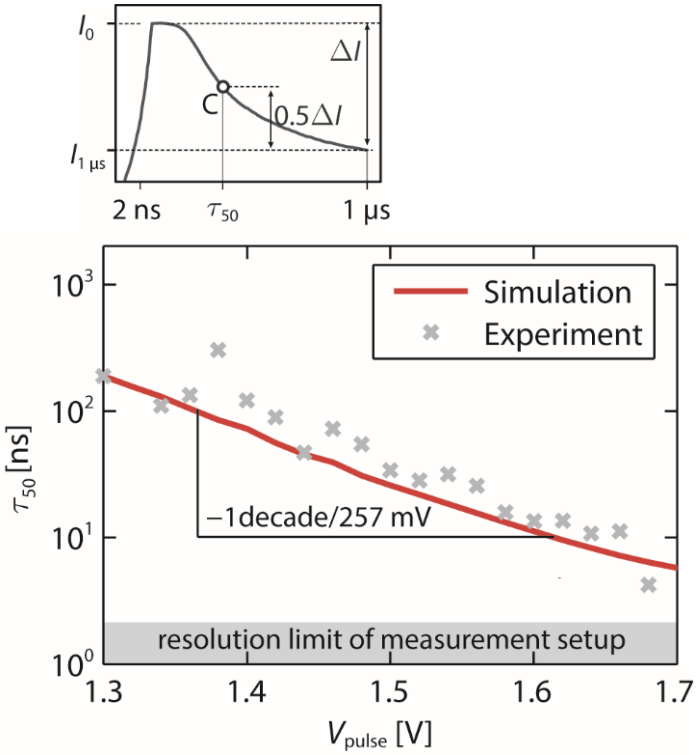

→ RESET kinetics can be explained by ion migration

A. Marchewka, S. Menzel et al., *Adv. Electron. Mater.*, vol. 2, no. 1, 1500233 (2016)

VCM RESET Kinetics III: Simulation Results (2D)

Transient current

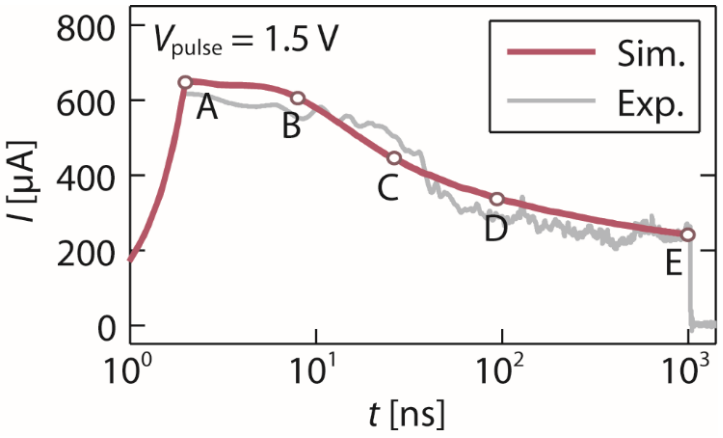

Temperature and vacancy distributions

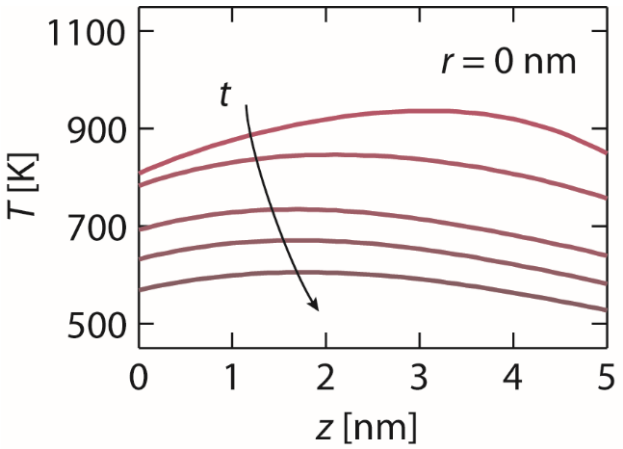

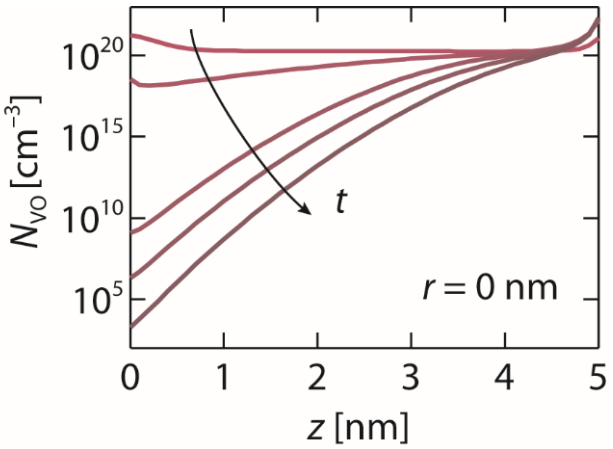

Transient vacancy current density

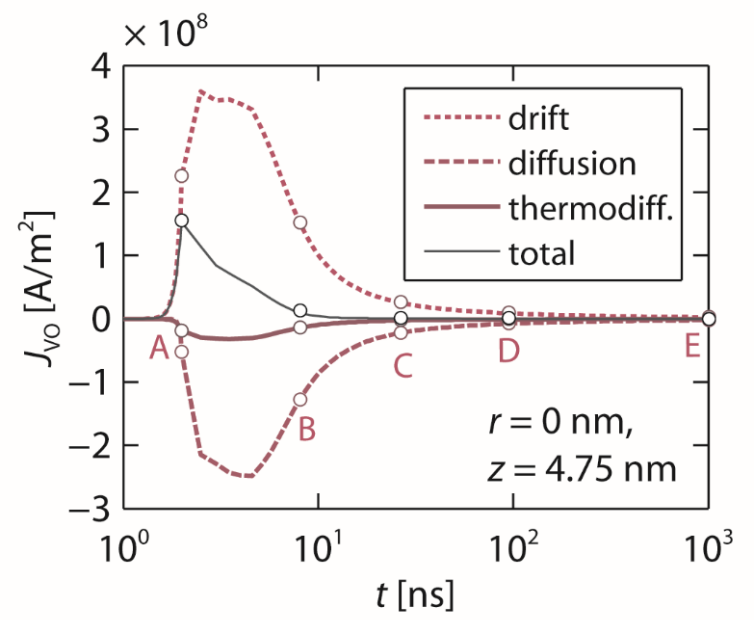

→ Gradual RESET due to balance between drift and diffusion

A. Marchewka, S. Menzel et al., *Adv. Electron. Mater.*, vol. 2, no. 1, 1500233 (2016)

Outline

- Motivation
- Electronic Transport in VCM Cells: A DFT-NEGF study
- Switching Variability of VCM Cells: Kinetic Monte Carlo Modeling
- Switching Dynamics of VCM Cells: Continuum Modeling
- **Towards Circuit Simulations: VCM Compact Models (JART)**
- Array Level Modeling
- Summary & Conclusion

JART VCM v1 Model I: Electrical Model

C. Bengel, S. Hoffmann-Eifert, S. Menzel et al., *IEEE T-CAS I*, vol. 67, no. 12, pp. 4618-4630 (2020)

Equivalent circuit diagram

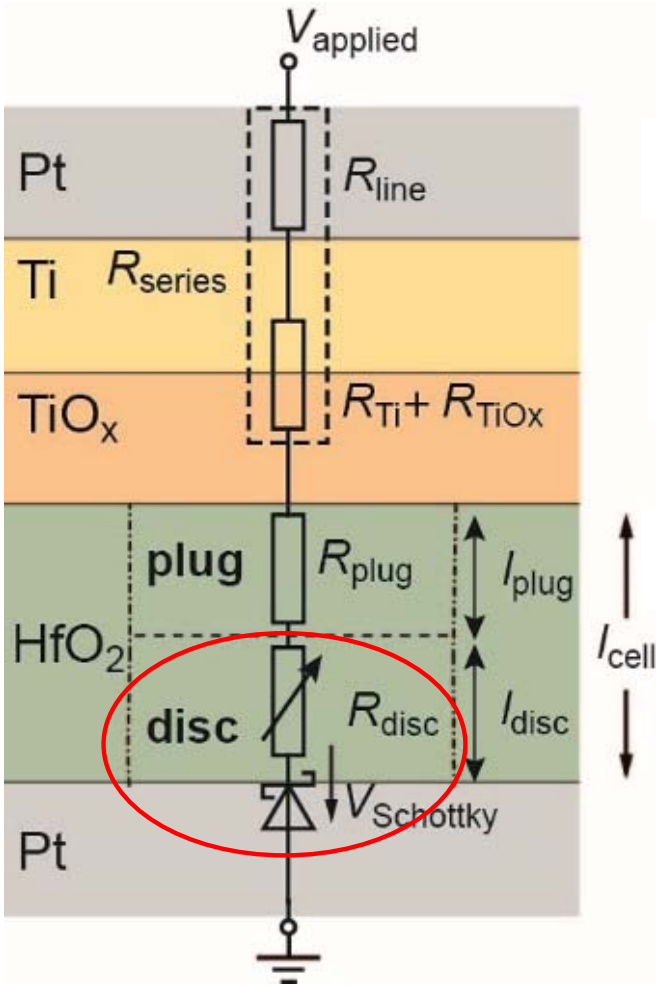

Series resistance

$$R_{series} = R_{line} + R_{TiOx}$$
$$= R_{TiOx} + R_0\left(1+\alpha_{line}R_0 I^2 R_{th,line}\right)$$

Plug resistance

$$R_{plug} = \frac{l_{cell} - l_{var}}{z_{Vo} e \mu_n A N_{plug}}$$

Disc resistance

$$R_{disc} = \frac{l_{var}}{z_{Vo} e \mu_n A N_{disc}}$$

MI interface ($V_{schottky}$)

Forward direction: Thermionic emission (TE)
Reverse direction: Thermionic field emission (TFE)

→ Conductance is defined by defect concentration close to the Pt electrode N_{disc}

JART VCM v1 Model II: Ionic Model

Driving force for is ionic current

$$\frac{\mathrm{d}N_{\mathrm{disc}}}{\mathrm{d}t} = -\frac{I_{\mathrm{ion}}}{ez_{\mathrm{Vo}}Al_{\mathrm{var}}}$$

$$I_{\mathrm{ion}} = ez_{\mathrm{Vo}}c_{\mathrm{Vo}}a_{\mathrm{Vo}}F_{\mathrm{limit}}A \cdot \left(\exp\left(-\frac{\Delta W_{\mathrm{min}}}{k_{\mathrm{B}}T}\right) - \exp\left(-\frac{\Delta W_{\mathrm{max}}}{k_{\mathrm{B}}T}\right)\right) = f\left(E,T\right)$$

Electric field

$$\mathrm{FB}: E = \left(V_{\mathrm{disc}} + V_{\mathrm{Schottky}} + V_{\mathrm{plug}}\right) / l_{\mathrm{cell}}$$

$$\mathrm{RB}: E = V_{\mathrm{disc}} / l_{\mathrm{disc}}$$

Joule heating

$$T = T_0 + R_{\mathrm{th,SET}} P_{\mathrm{device}} \quad \text{SET}$$

$$T = T_0 + R_{\mathrm{th,RESET}} P_{\mathrm{device}} \quad \text{RESET}$$

Ion in periodic lattice

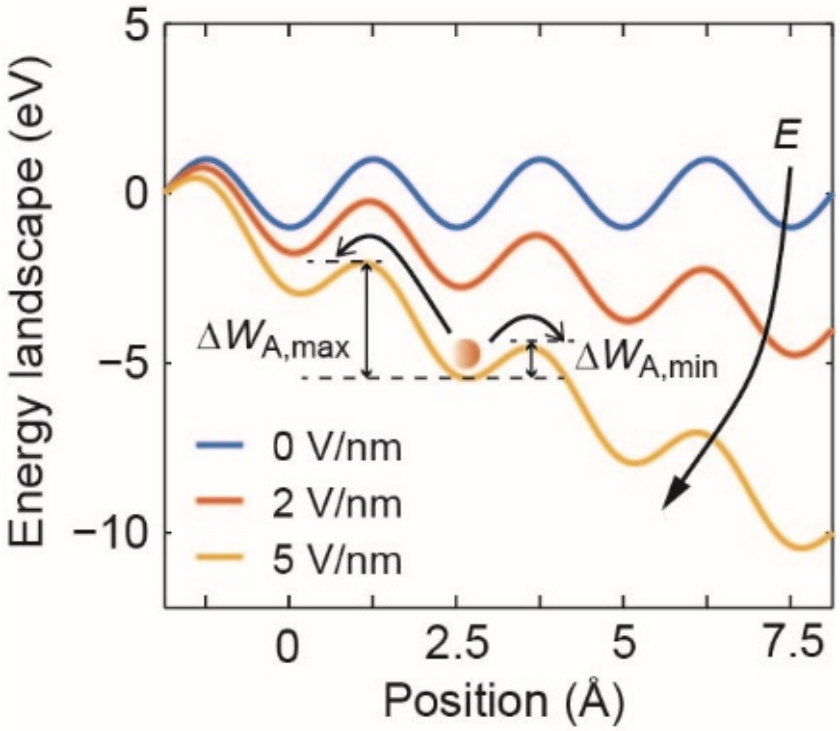

S. Menzel et al., *Faraday Discussions* vol. 213, pp. 197-213 (2018)

A. Genreith-Schriever, et al., *Phys. Rev. B* vol. 94, no. 22, pp. 224304 (2016)

Physical Origin of the Switching Variability

PEEM analysis of $SrTiO_3$-based cells

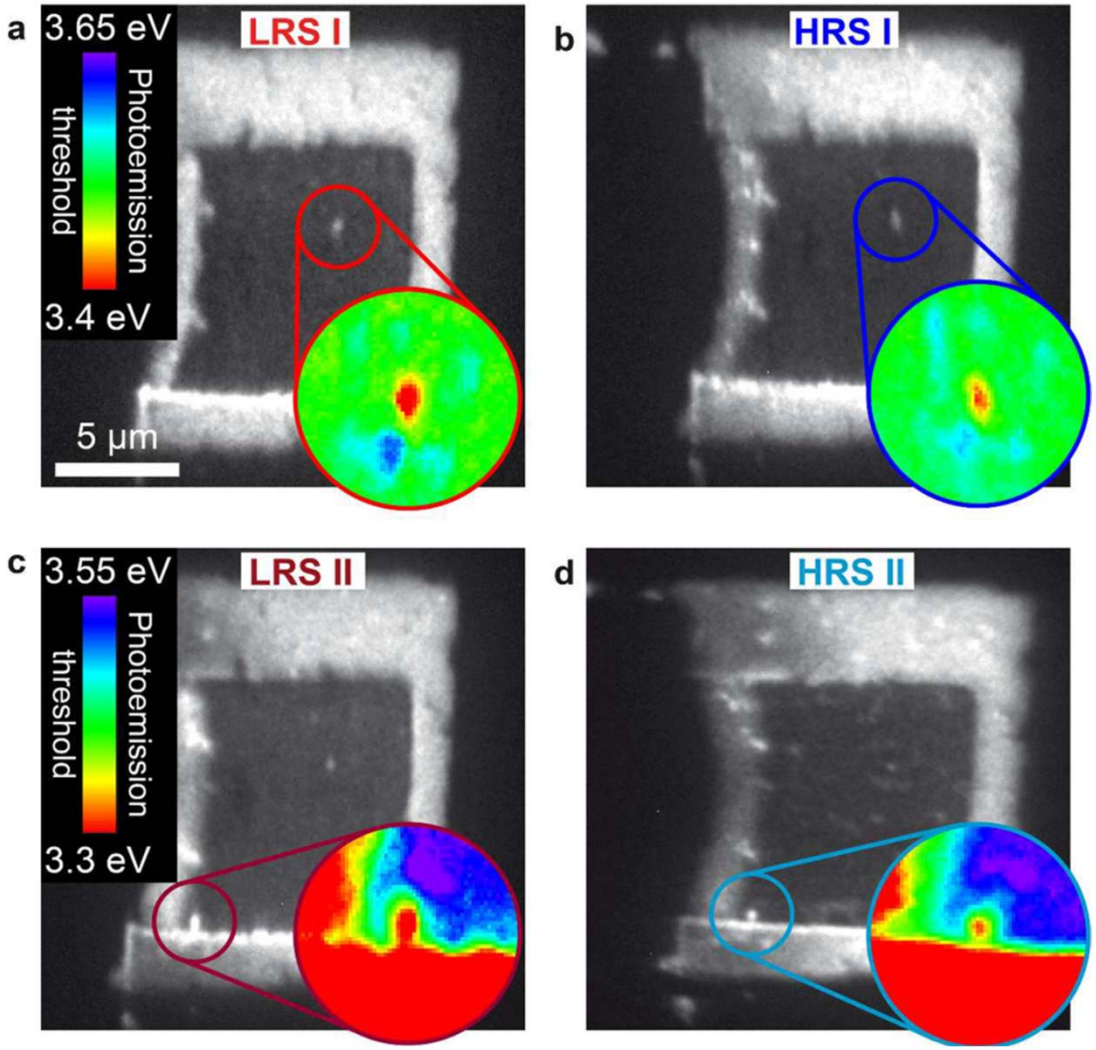

→ Parallel growth of multiple filaments

→ One filament „wins“ during SET

→ Variability due to change of filament location and geometry

C. Baeumer, R.Dittmann, et al., *ACS Nano,* vol. 11, no. 7, pp. 6921-6929 (2017)

JART VCM v1: Modeling the Switching Variability I

→ Variability due change in filament properties

Device-to-device variability

Parameter are chosen randomly from a truncated Gaussian distribution

- Minimum disc concentration $N_{disc,min}$
- Maximum disc concentration $N_{disc,max}$
- Filament radius r
- Disc length l

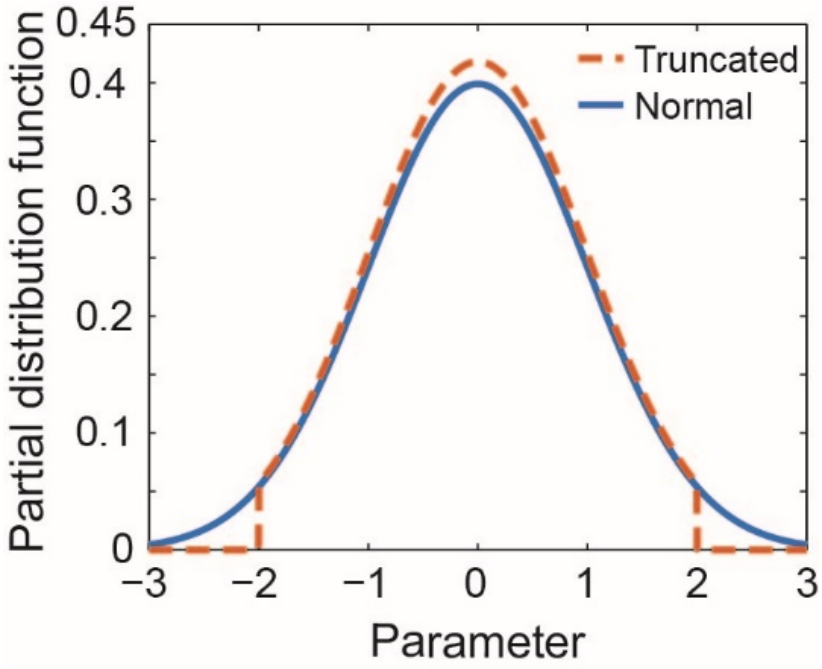

C. Bengel, S. Hoffmann-Eifert, S. Menzel et al.,
IEEE T-CAS I, vol. 67, no. 12, pp. 4618-4630 (2020)

JART VCM v1: Modeling the Switching Variability II

Cycle-to-cycle variability

Random walk algorithm is used to change the parameters from c2c

$$\xi_k = \xi_{k-1}\left(1 \pm \Delta\xi_{\max} \cdot P\right) \qquad P \in (0,1)$$

Change of *r*, and *l* depends on N_{disc}

SET

$$r_{\text{var}} = r_{\text{old}} + \left(r_{\text{new}} - r_{\text{old}}\right)\left(\frac{N_{\text{disc}} - N_{\text{disc,old}}}{N_{\text{disc,max,var}} - N_{\text{disc,old}}}\right)$$

$$l_{\text{var}} = l_{\text{old}} + \left(l_{\text{new}} - l_{\text{old}}\right)\left(\frac{N_{\text{disc}} - N_{\text{disc,old}}}{N_{\text{disc,max,var}} - N_{\text{disc,old}}}\right)$$

RESET

$$r_{\text{var}} = r_{\text{old}} + \left(r_{\text{new}} - r_{\text{old}}\right)\left(\frac{N_{\text{disc,old}} - N_{\text{disc}}}{N_{\text{disc,old}} - N_{\text{disc,min,var}}}\right)$$

$$l_{\text{var}} = l_{\text{old}} + \left(l_{\text{new}} - l_{\text{old}}\right)\left(\frac{N_{\text{disc,old}} - N_{\text{disc}}}{N_{\text{disc,old}} - N_{\text{disc,min,var}}}\right)$$

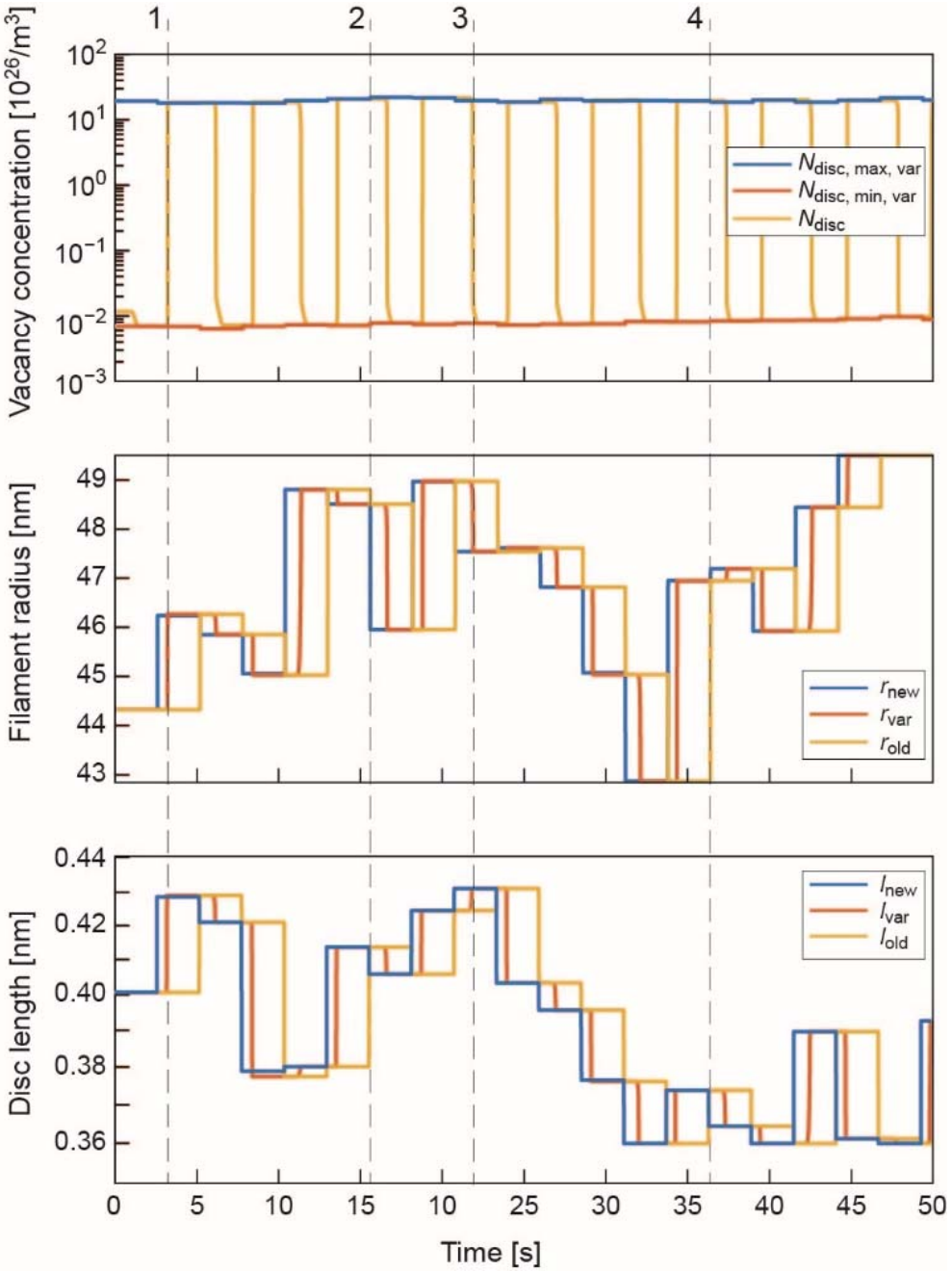

JART VCM v1: Modeling Read Noise

Physical Origin

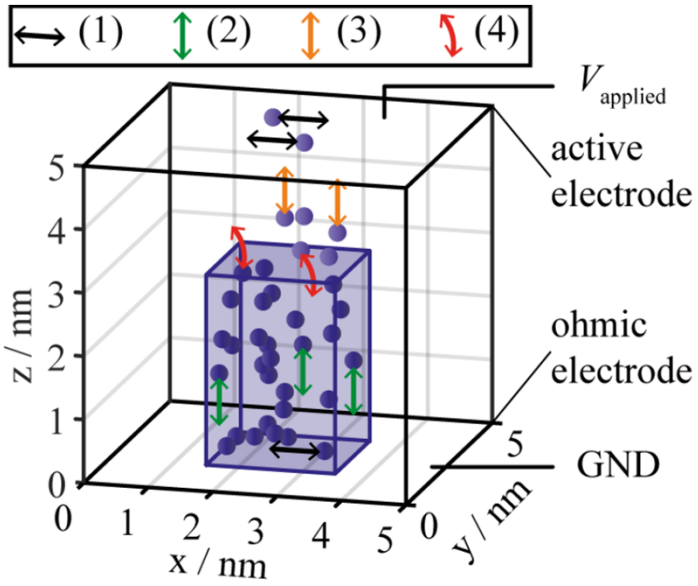

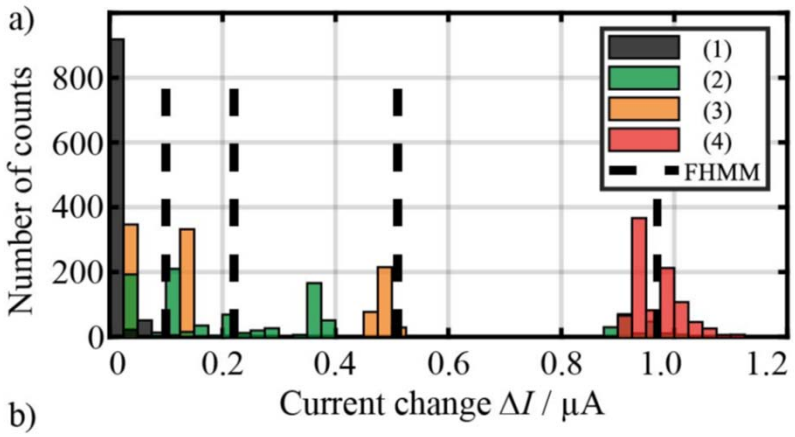

Read instability model

→ Most important jump between plug to disc

→ Change of N_{disc} by ±1, ±2 defects

Implemented using state machine

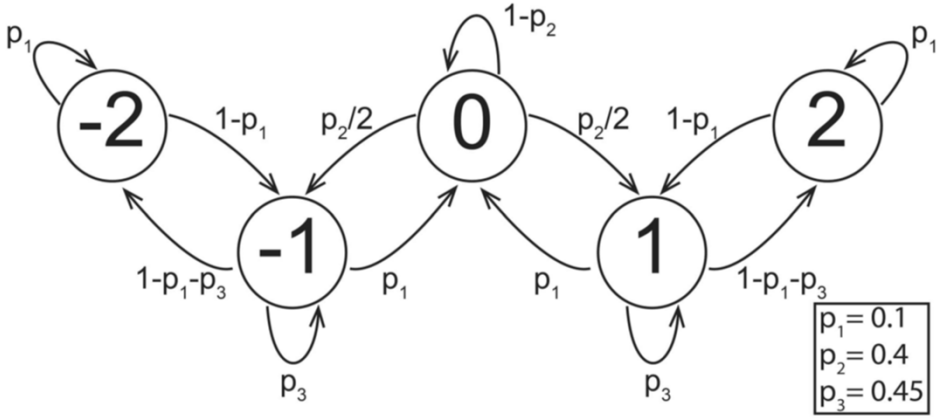

S. Wiefels, S. Menzel et al., *IEEE T-ED*, vol. 67, no. 10, pp. 4208-4215 (2020)

Compact Modeling of SET Dynamics

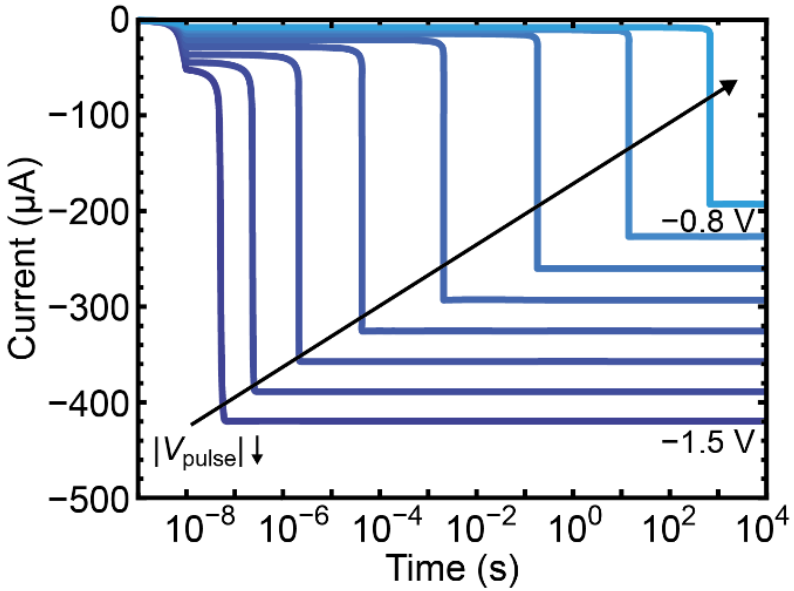

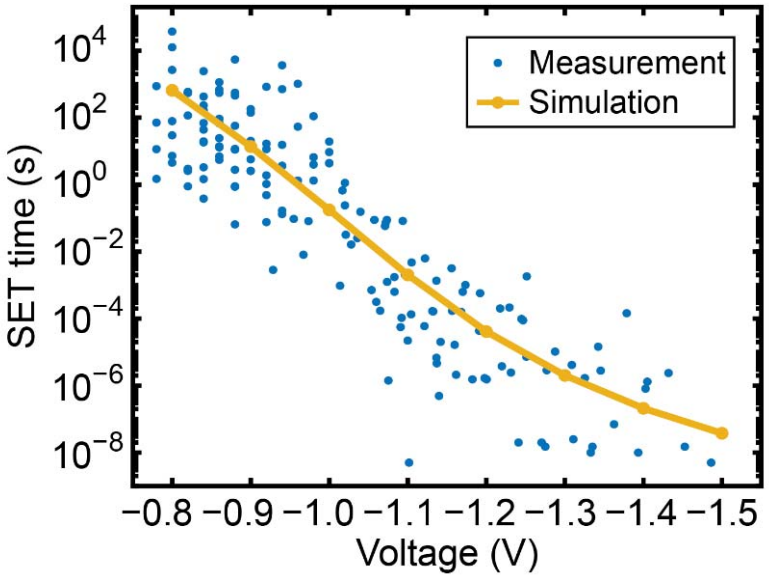

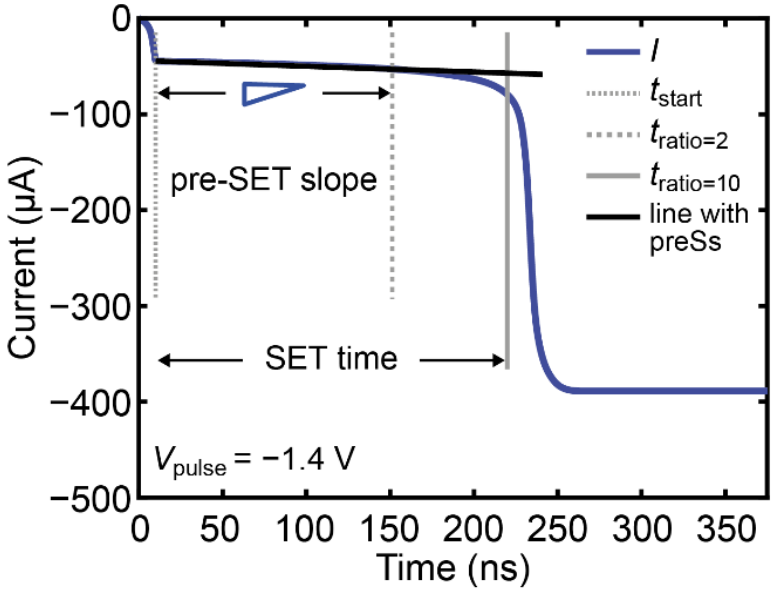

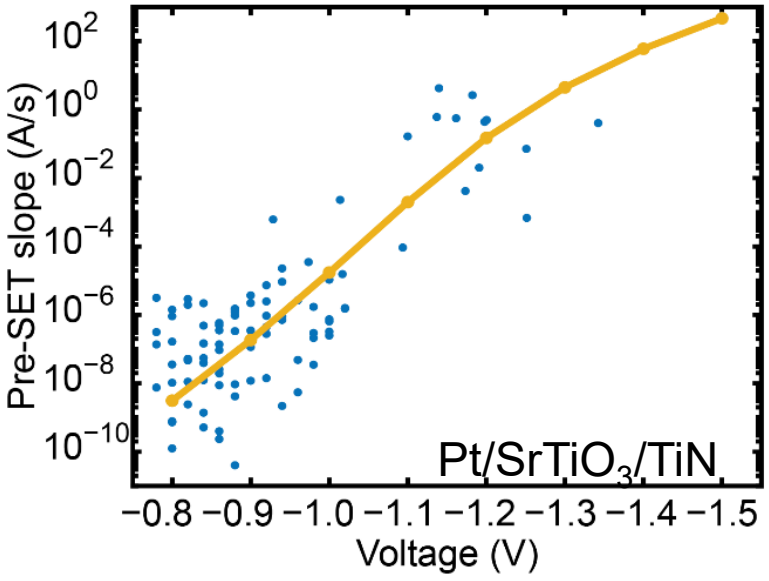

K. Fleck, S. Menzel et al., *Phys. Rev. Applied,* Vol. 6, No. 6, 064015, 2016
C. La Torre, PhD dissertation, 2019, RWTH Aachen University

Compact Modeling of RESET Dynamics

RESET transients

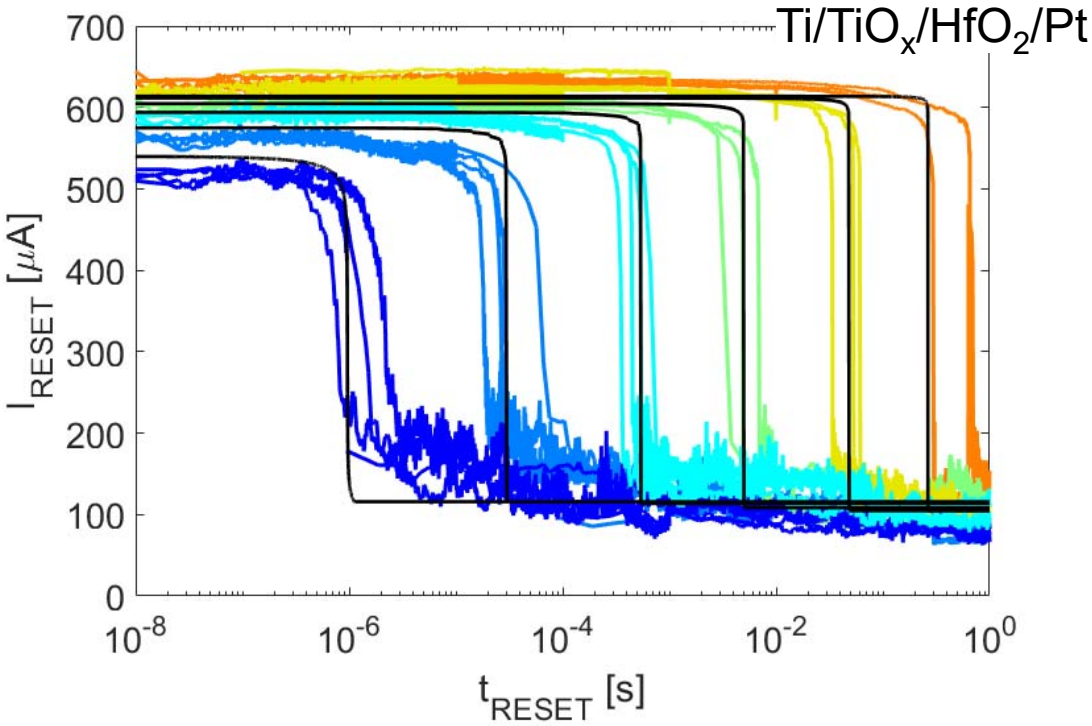

RESET kinetics

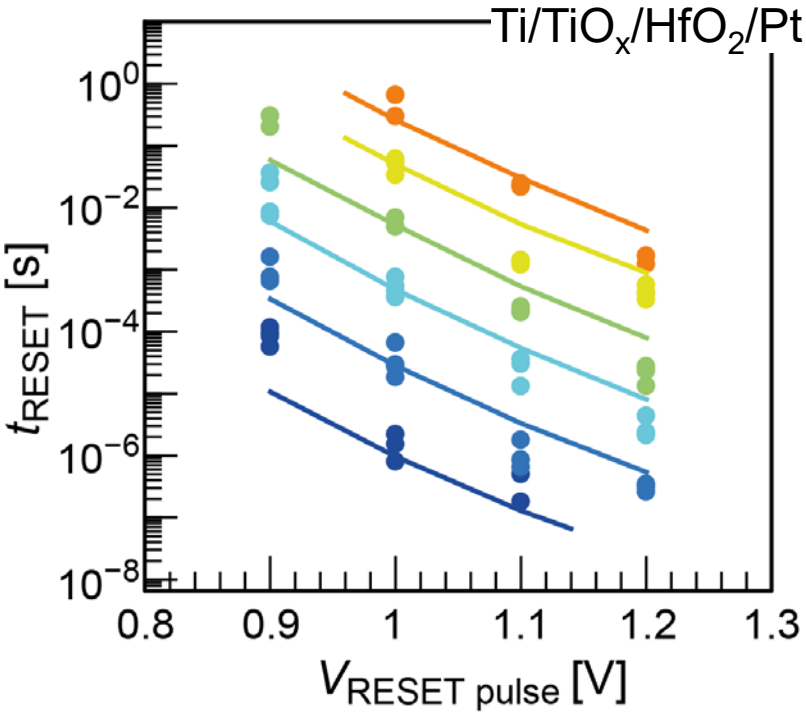

→ Voltage-divider between series resistance and actual device leads to strong state-dependence

F. Cüppers, S. Menzel et al., *APL Materials* vol. 7, no. 9, pp. 91105 (2019)

Switching Variability I

C. Bengel, S. Menzel et al., *IEEE T-CAS I*, vol. 67, no. 12, pp. 4618-4630 (2020)

Experiment

$Ti/TiO_x/HfO_2/Pt$

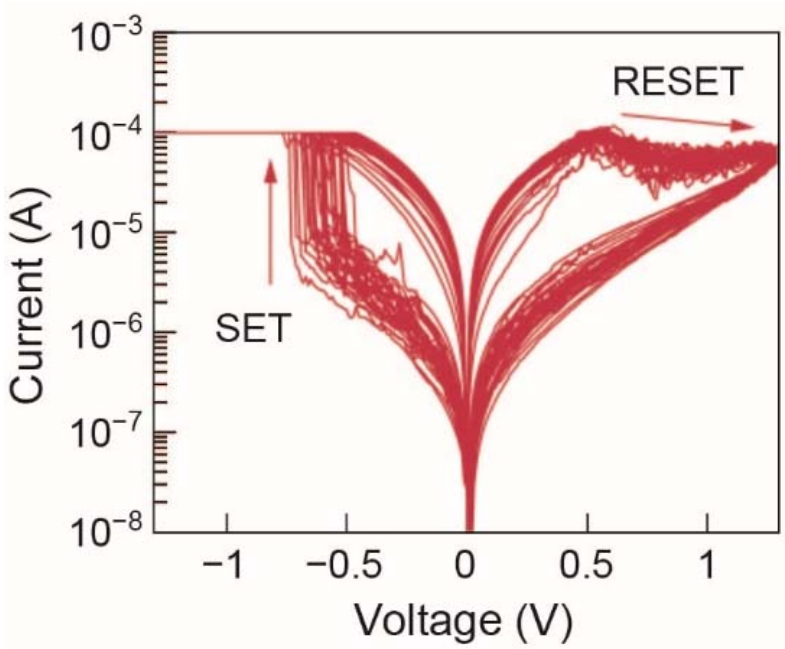

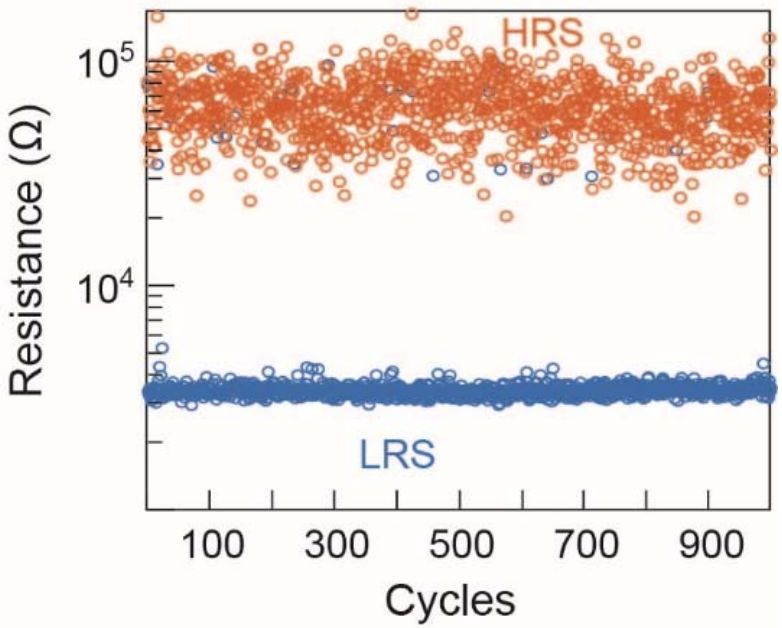

Simulation

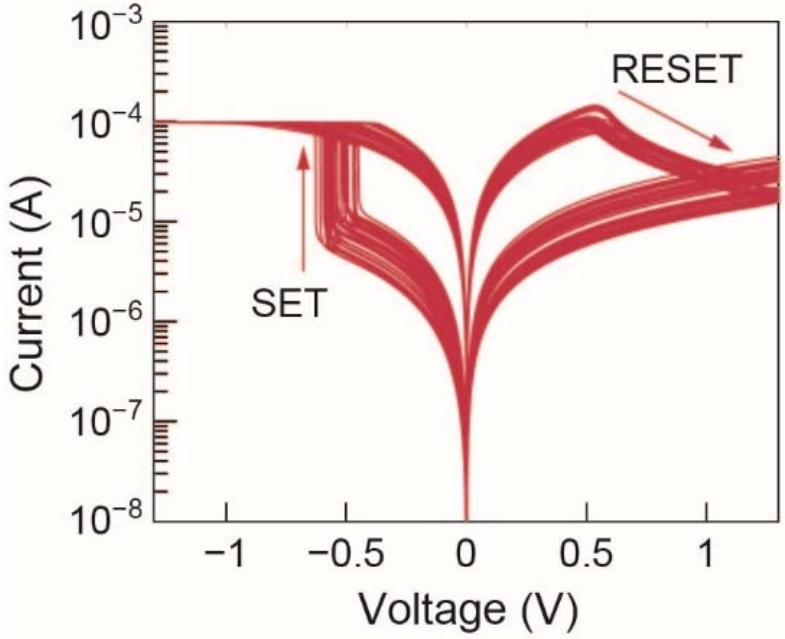

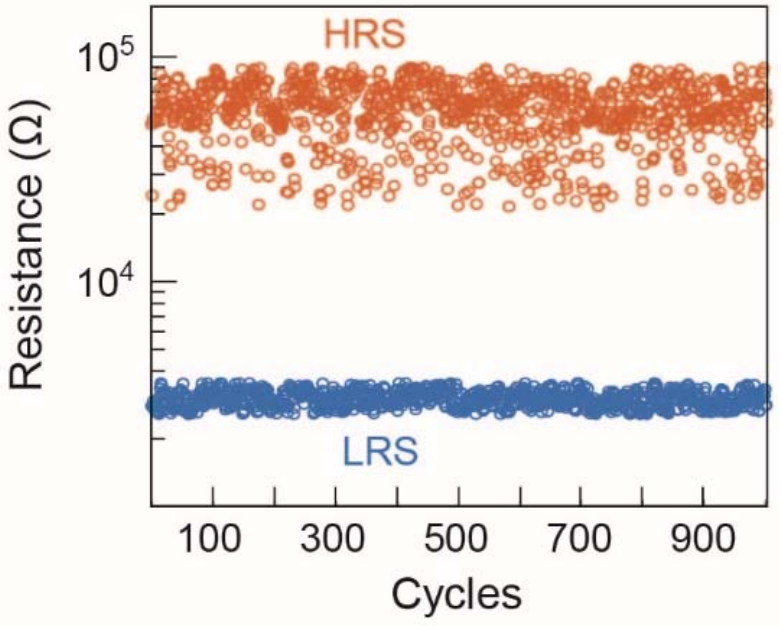

Switching Variability II

C. Bengel, S. Menzel et al., *IEEE T-CAS I*, vol. 67, no. 12, pp. 4618-4630 (2020)

Experiment

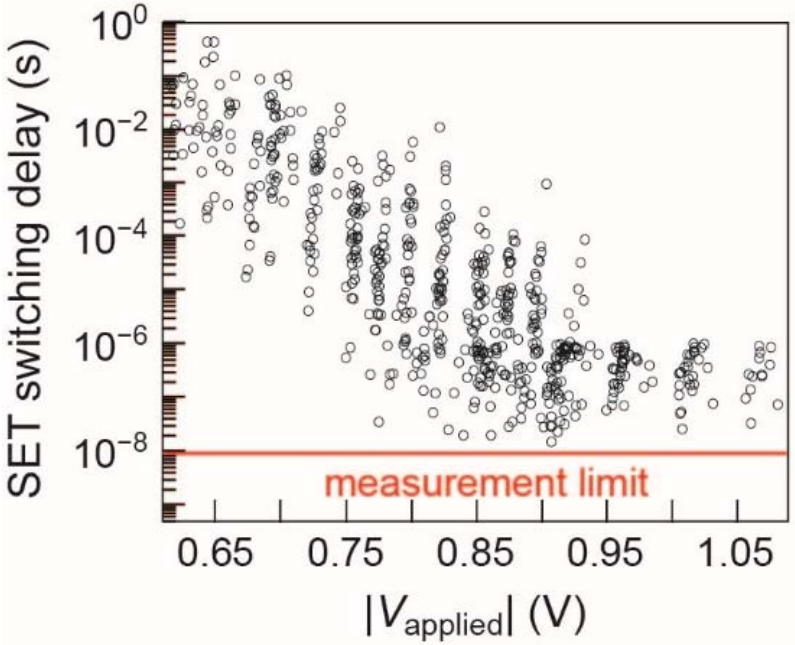

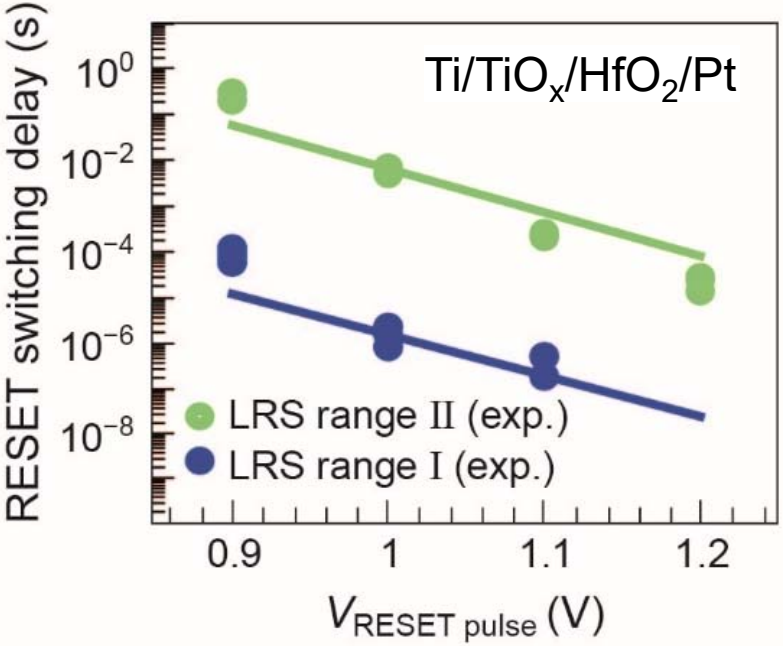

Simulation

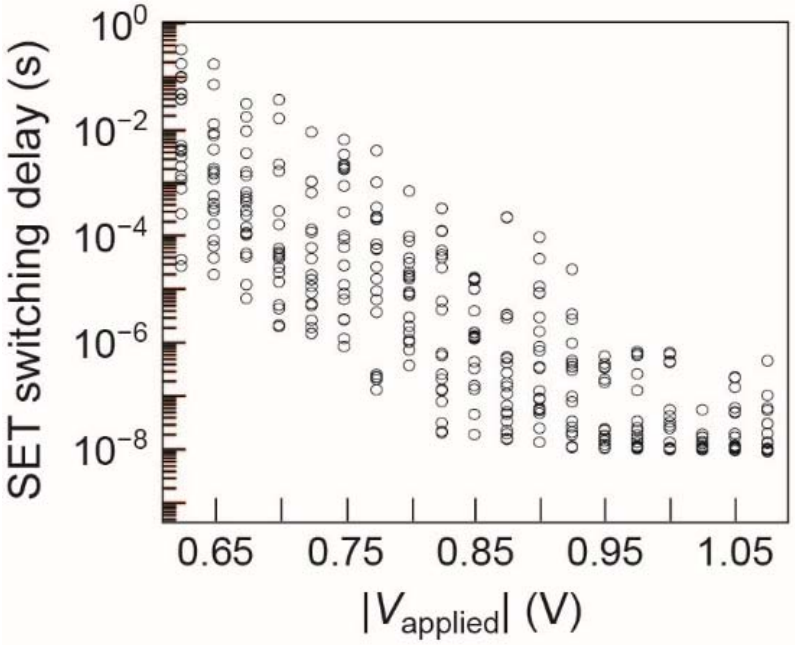

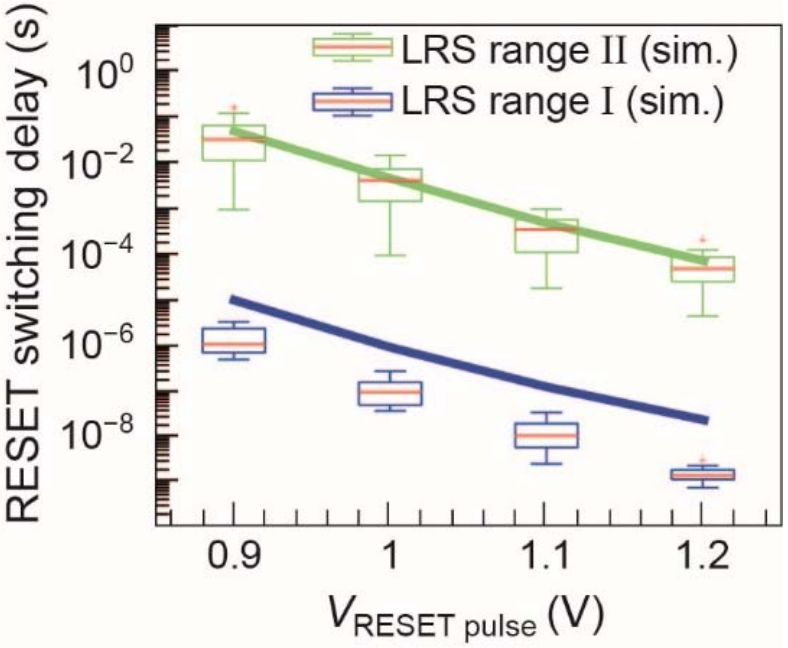

Simulation of Read Instability: JART VCM 1b

Simulated *I-t* curve

Observed current jumps similar to experimental ones

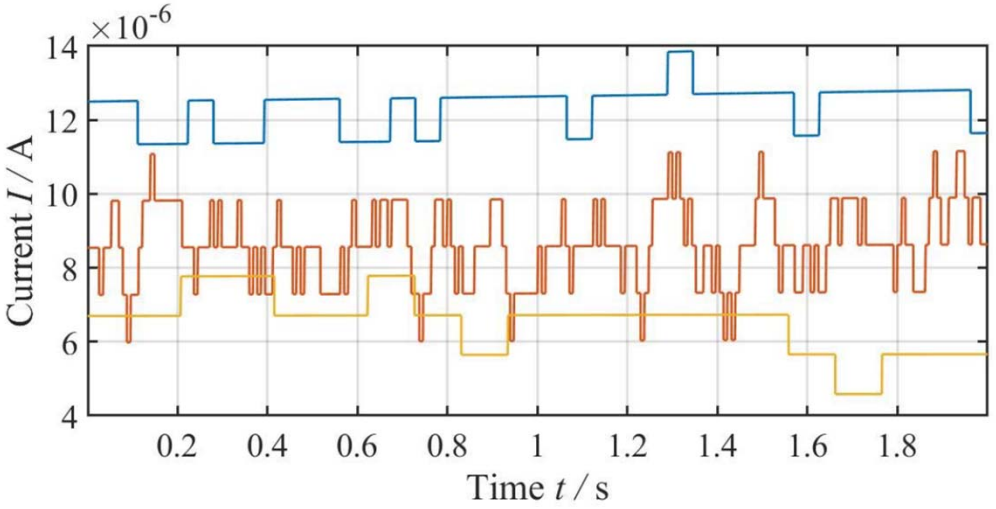

Simulated and experimental read distribution

- Log-normal distribution observed
- Log-normal distribution recovers after shaping experiment

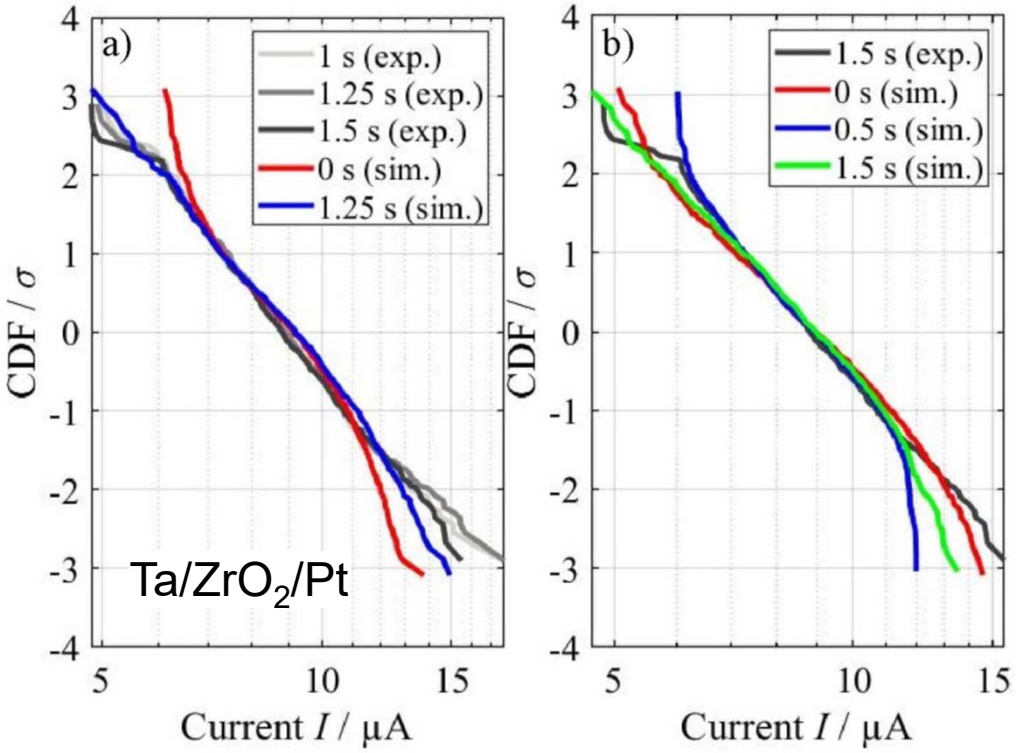

S. Wiefels, S. Menzel et al., *IEEE T-ED*, vol. 67, no. 10, pp. 4208-4215 (2020)

JART VCM: A 1D Kinetic Monte Carlo Approach

Based on ***JART VCM 1.0*** Compact model

Ion movement

- *Mott-Gurney law* extended by KMC method
- $V_{Ö}$ jump: plug ↔ disc

$$R^{f,r} = \nu_0 \times \exp\left(-\frac{\Delta W_A^{f,r}}{k_B T}\right)$$

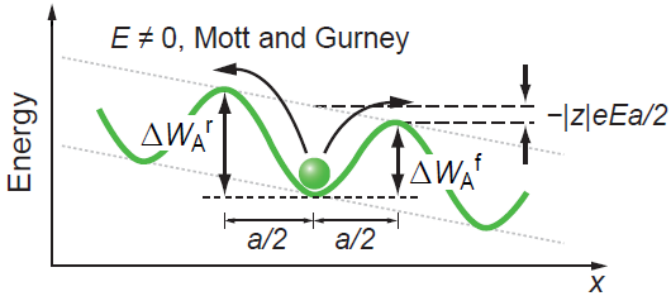

- Weighted, random process selection
- Time update

$$t_{jump} = \frac{\ln(rand)}{R^f + R^r}$$

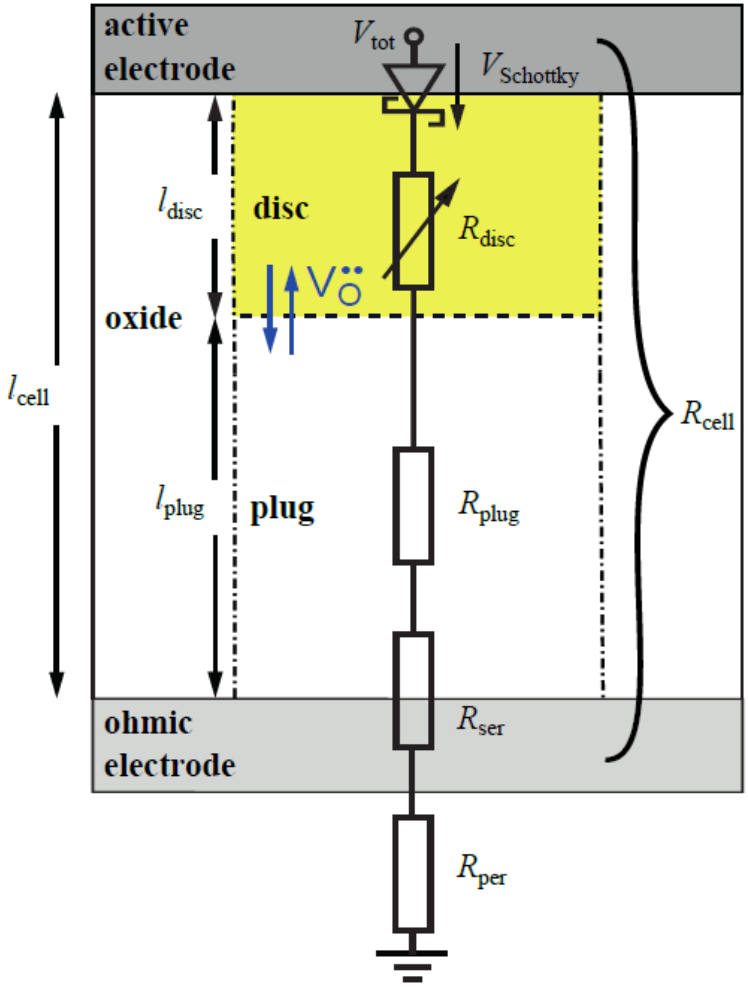

N. Kopperberg, S. Menzel et al., *IEEE Access,* vol. 10, pp. 122696 – 122705 (2022)

Stuck-at-LRS Failure in Test Chips

Endurance Data on 2 Mbit Cells

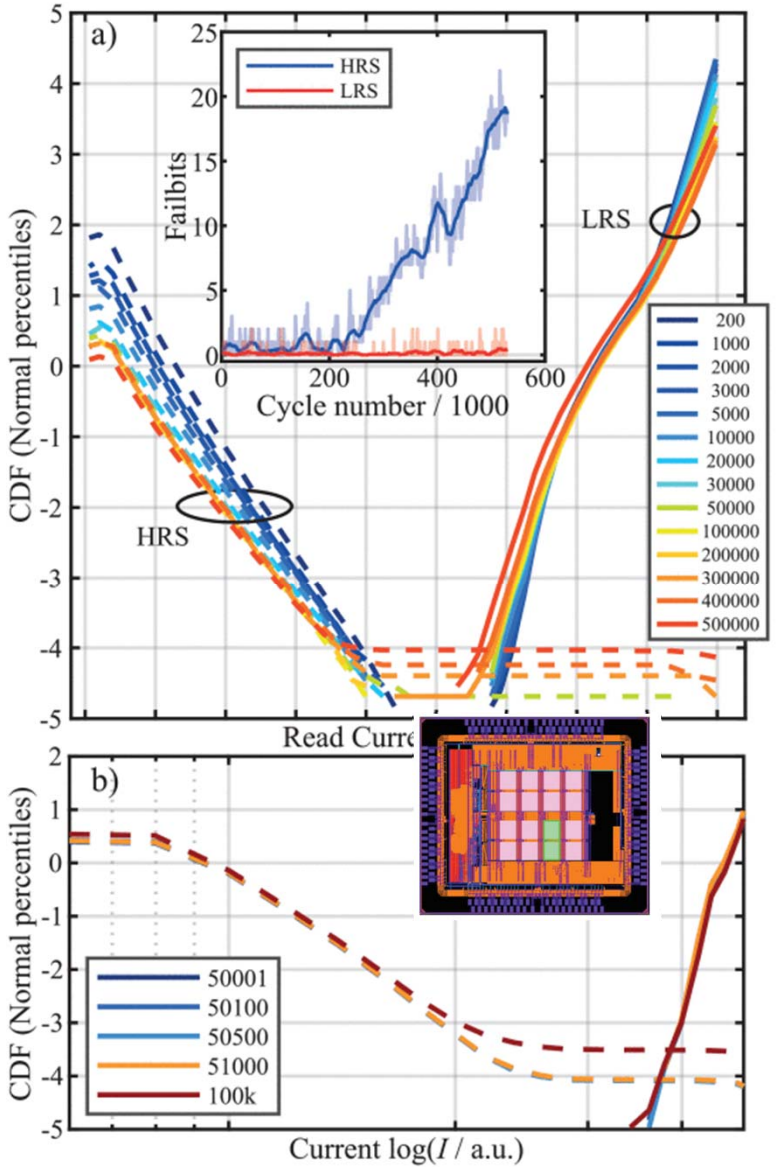

Simulated Failure using 1D KMC Model

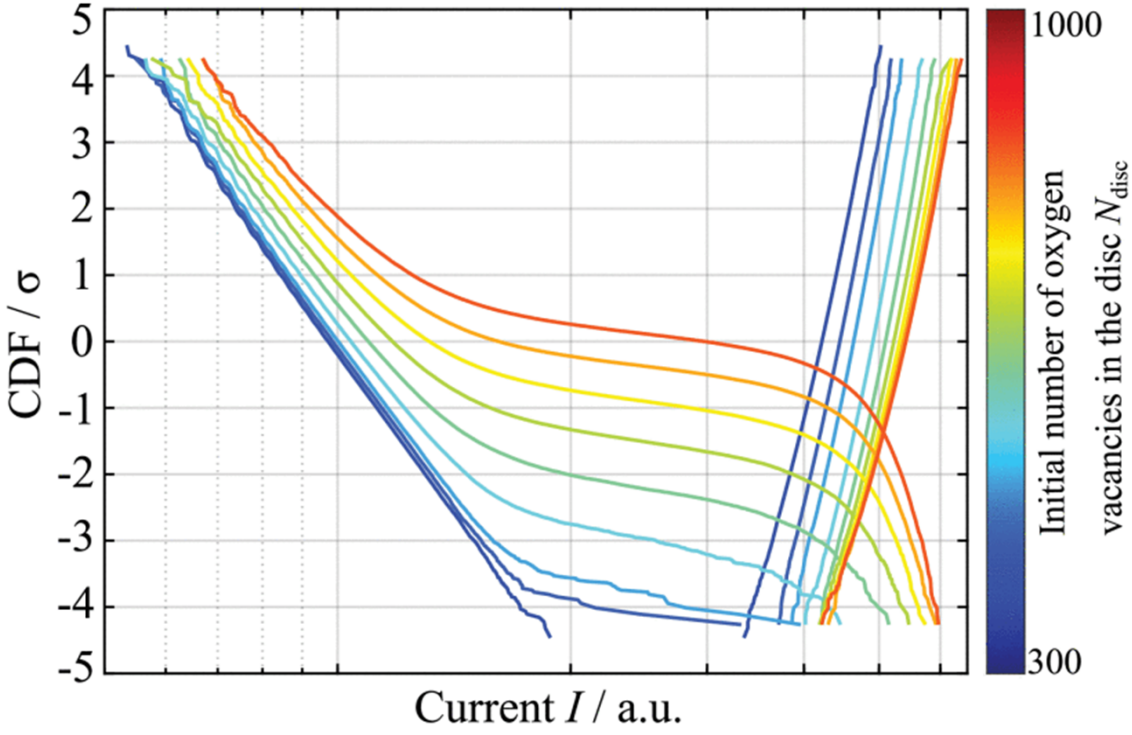

→ Decreased RESET probability due to voltage divider effect

N. Kopperberg, S. Menzel et al., *IEEE Access*, vol. 10, pp. 122696 – 122705 (2022)

JART VCM: Further Model Simplification I

Fitting the state equation and state-dependent's Ohm's law using logistic functions

$$I = f\left(N_{\text{disc}}, V_{\text{app}}, r_{\text{fil}}, l_{\text{disc}}\right)$$

$$\frac{\mathrm{d}N_{\text{disc}}}{\mathrm{d}t} = f\left(N_{\text{disc}}, V_{\text{app}}, r_{\text{fil}}, l_{\text{disc}}\right)$$

→ Higher number of fitting parameters
→ Parameters purely empirical

V. Ntinas, S. Menzel, R. Tetzlaff et al.
IEEE TCAS-II, vol. 14, no. 8, 2473 – 2477 (2023)

V. Ntinas, S. Menzel, R. Tetzlaff et al.,
Int. Conf. *SMACD'23* (2023)

Device current

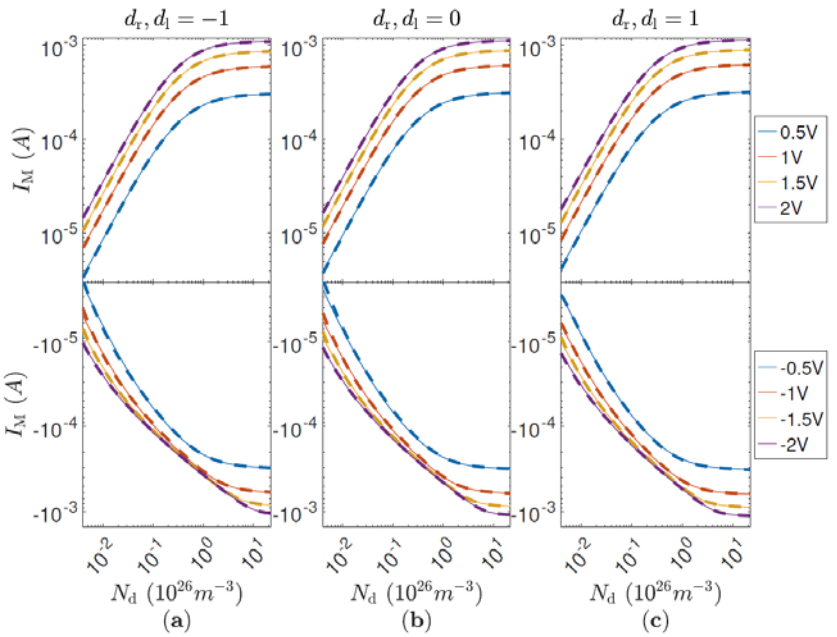

Dynamic route map

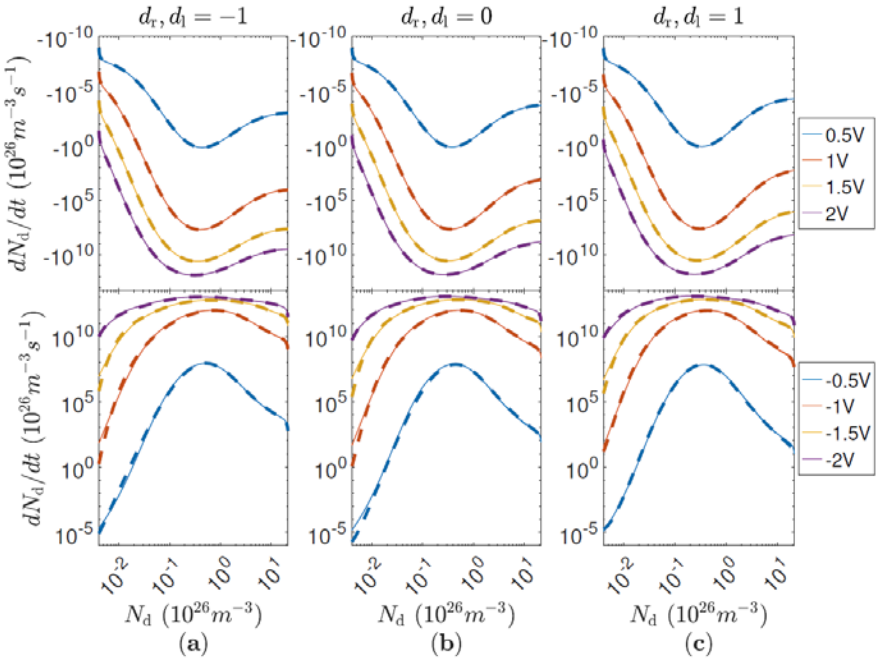

JART VCM: Further Model Simplification II

Simulation time scaling over the number of parallel memristors

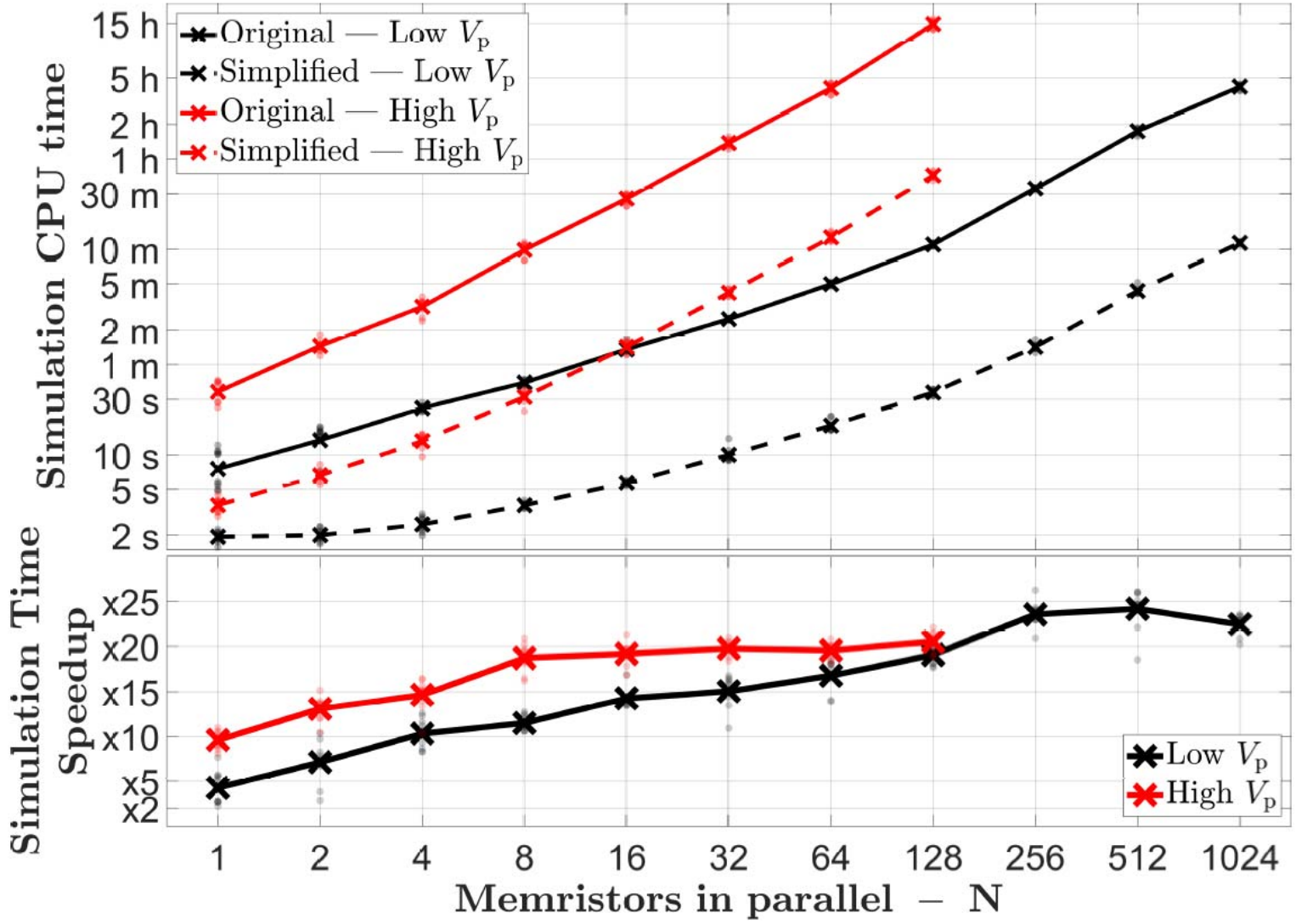

V. Ntinas, S. Menzel, R. Tetzlaff et al., Int. Conf. *SMACD'23*

A Data-Driven Modeling Approach

Real-world measurement data

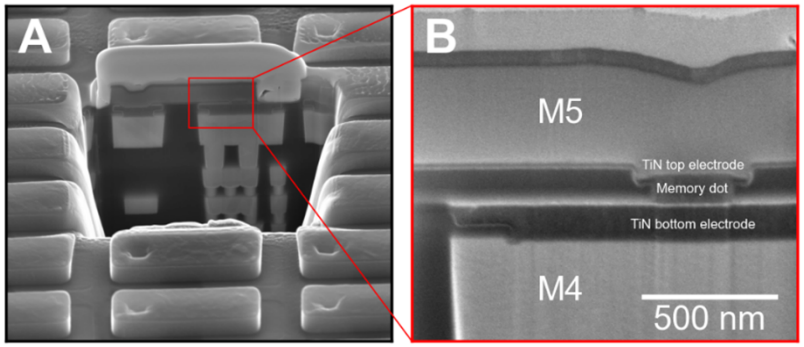

Training

I-V cycle measurements

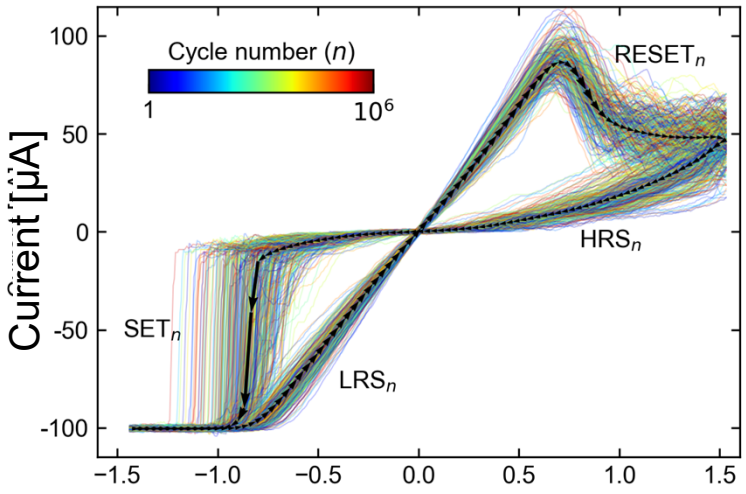

Parameter extraction

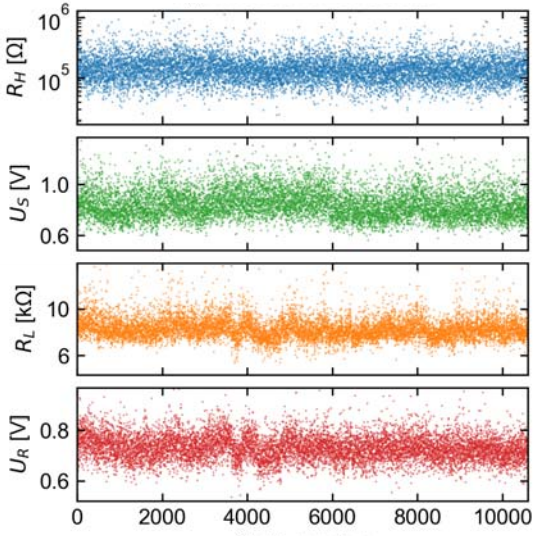

Generative device model

×1 billion devices in memory!

Parameter generation

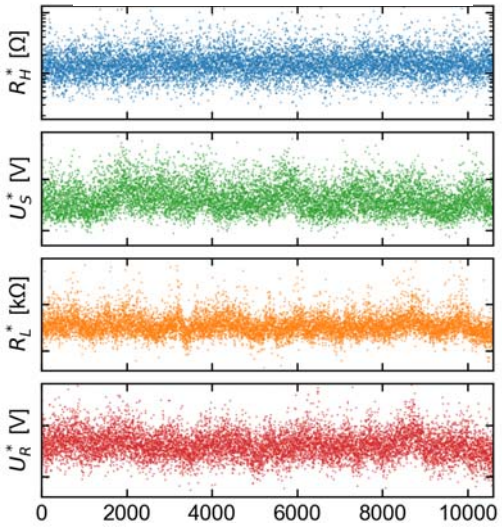

I-V cycle reconstruction

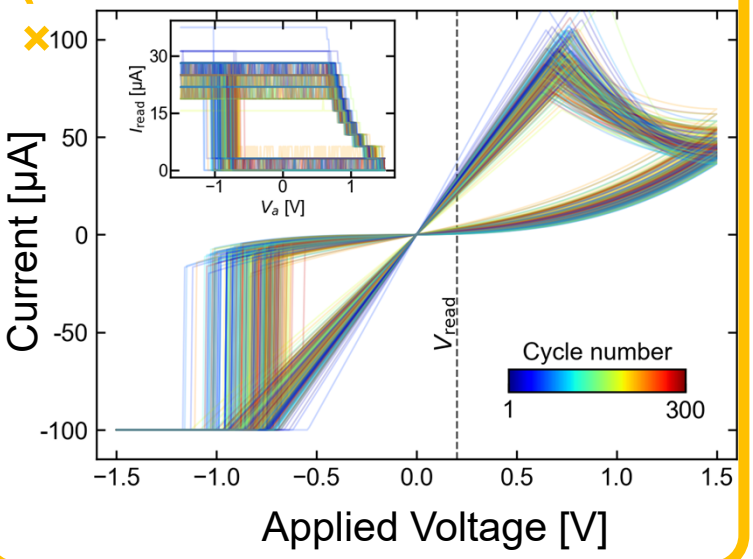

Hennen et al, *Frontiers in Neuroscience*, vol. 16, p. 941753, 2022

Outline

- Motivation
- Electronic Transport in VCM Cells: A DFT-NEGF study
- Switching Variability of VCM Cells: Kinetic Monte Carlo Modeling
- Switching Dynamics of VCM Cells: Continuum Modeling
- Towards Circuit Simulations: VCM Compact Models (JART)
- **Array Level Modeling**
- Summary & Conclusion

Modeling Thermal Crosstalk

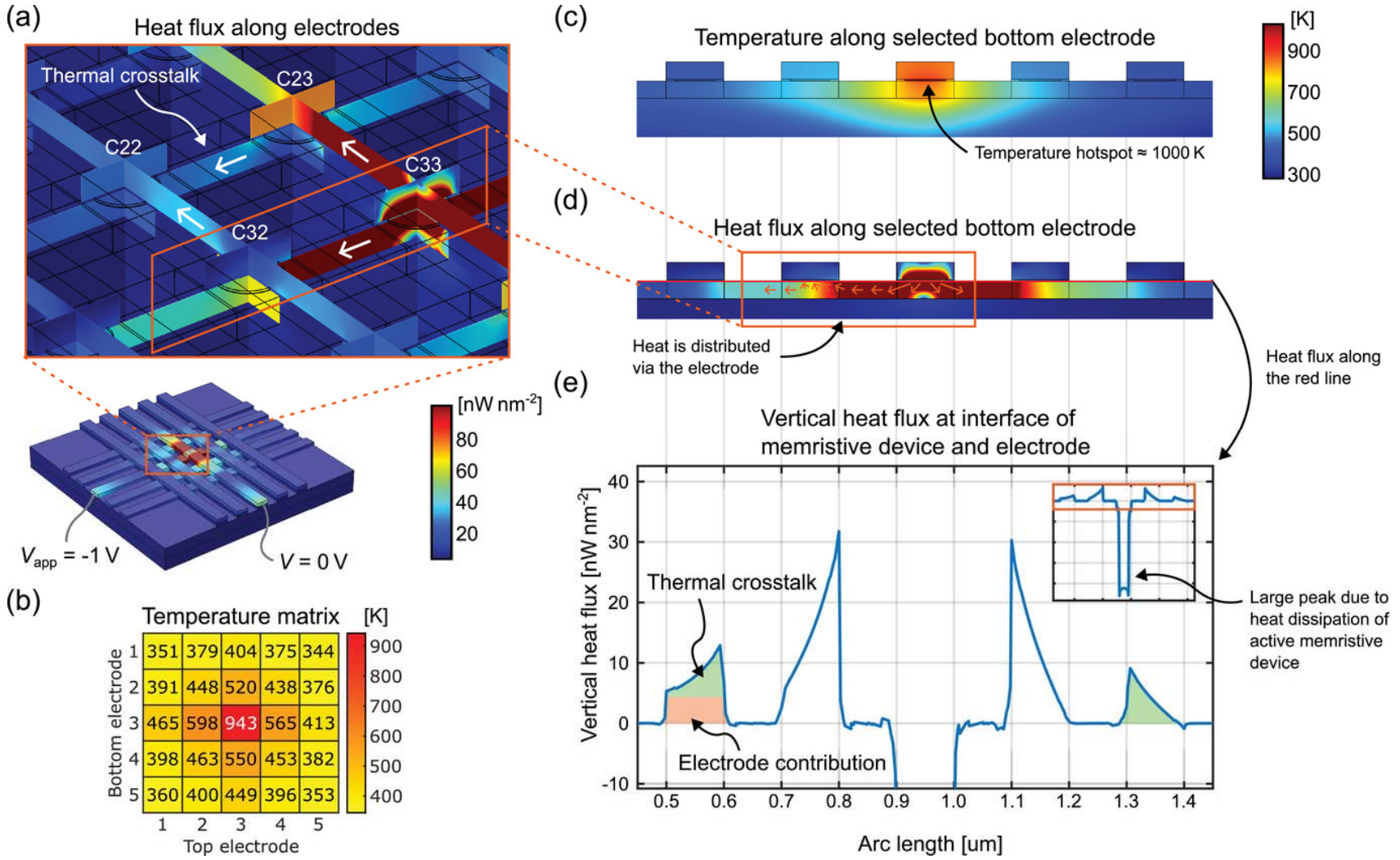

→ Thermal crosstalk via electrodes

D. Schön, S. Menzel et al., *Adv. Funct. Mater.,* https://doi.org/10.1002/adfm.202213943 (2023)

Array-level Simulations including Thermal Crosstalk

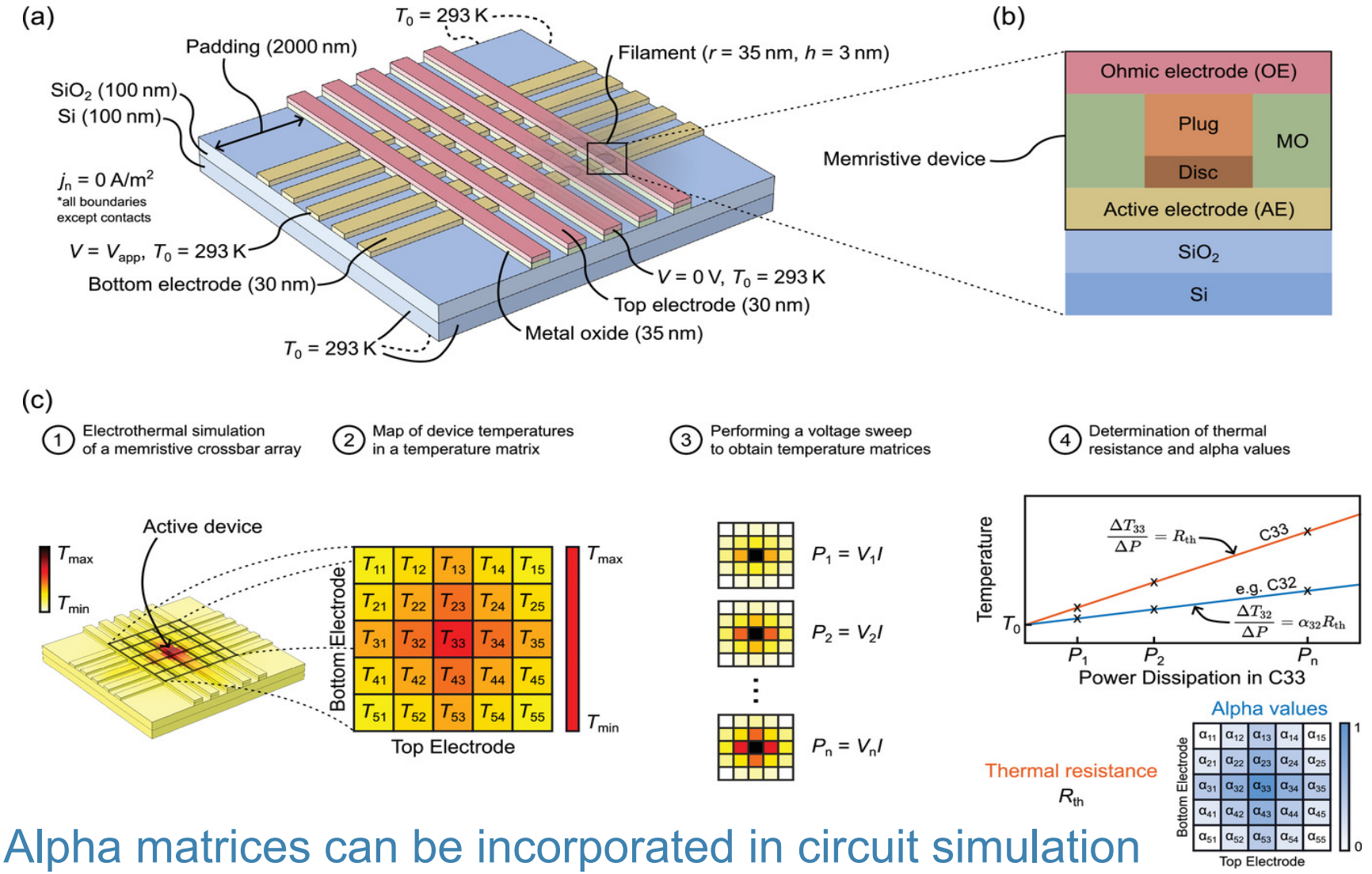

→ Alpha matrices can be incorporated in circuit simulation

D. Schön, S. Menzel et al., *Adv. Funct. Mater.,* https://doi.org/10.1002/adfm.202213943 (2023)

F. Staudigl, S. Menzel, R. Leupers et al., *DATE 2022*

Spatio-temporal Correlations in Crossbar Arrays

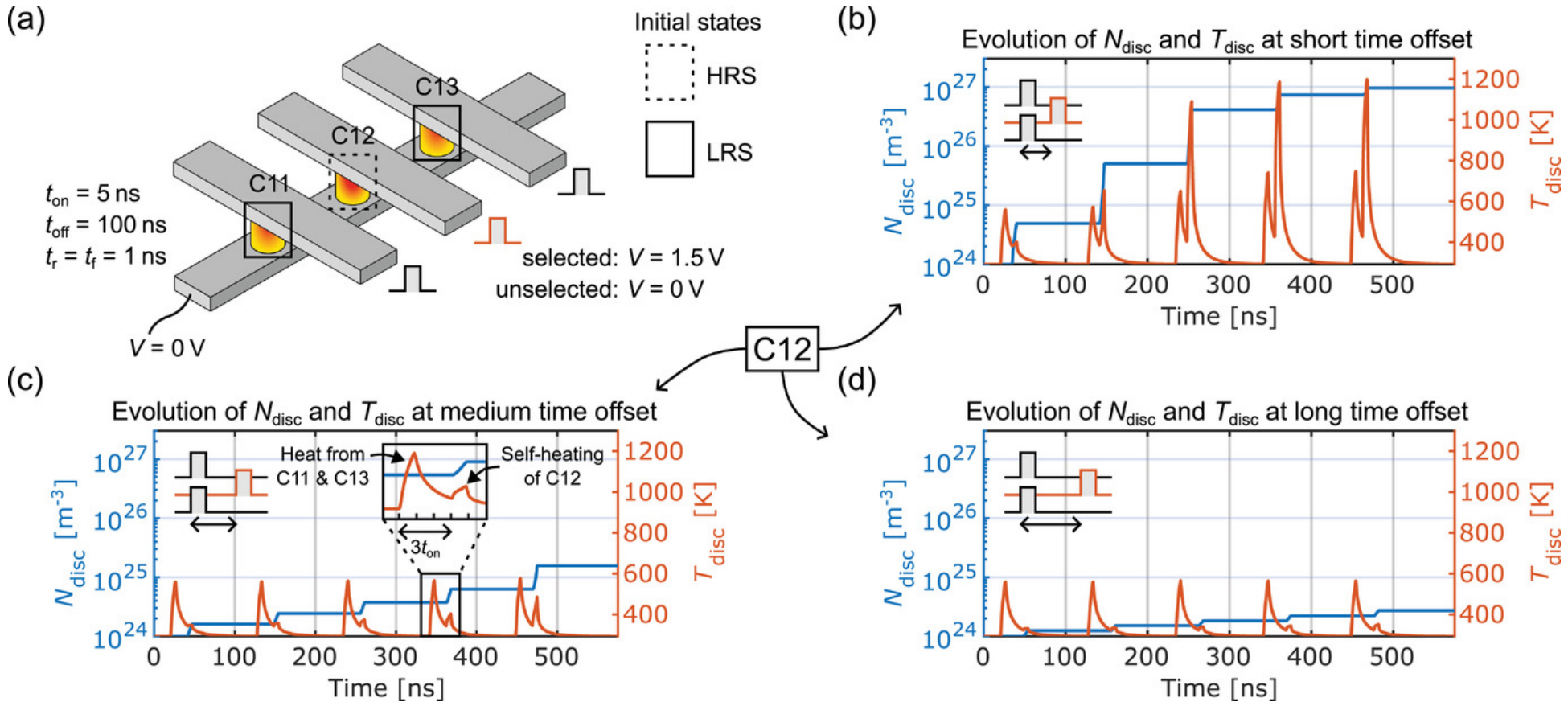

→ For Δt smaller t_{RC} adjacent cells can switch

D. Schön, S. Menzel et al., *Adv. Funct. Mater.,* https://doi.org/10.1002/adfm.202213943 (2023)

Outline

- Motivation
- Electronic Transport in VCM Cells: A DFT-NEGF study
- Switching Variability of VCM Cells: Kinetic Monte Carlo Modeling
- Switching Dynamics of VCM Cells: Continuum Modeling
- Towards Circuit Simulations: VCM Compact Models (JART)
- Array Level Modeling
- **Summary & Conclusion**

Summary

Electronic Transport in VCM Cells is Injection Limited
Type I conduction: injection into conduction band
Type II conduction: injection into defect levels

Switching Variability
Stochasticity causes only minor part of the variability
(major contribution is state-dependence of switching)
Read instability due to random ionic jumps into the “gap” region
Multi-domain model could explain different time regimes of ionic noise and retention

Switching Dynamics
Abrupt SET in filamentary VCMs due to a thermal runaway
Gradual RESET due to a non-isothermal drift-diffusion balance

Compact Modeling
JART Models including variability presented

Array Level Modeling
Combination of FEM and compact modeling → extraction of crosstalk

MemristTec

Funded by DFG Deutsche Forschungsgemeinschaft German Research Foundation

Thank you for your attention!

www.emrl.de/JART.html

NEUROTEC

FKZ:
16ES1133K
16ES1134

GEFÖRDERT VOM Bundesministerium für Bildung und Forschung

SFB 917 Nanoswitches